

1 **Response of catchment water storage capacity to the**
2 **prolonged meteorological drought and asymptotic**
3 **climate variation**

4

5 **Jing Tian¹, Zhengke Pan^{2,1}, Shenglian Guo^{1*}, Jiabo Yin¹, Yanlai Zhou¹, Jun Wang¹**

6

7 ¹State Key Laboratory of Water Resources and Hydropower Engineering Science,

8 Wuhan University, Wuhan 430072, China

9

10 ²Changjiang Institute of Survey, Planning, Design and Research, Wuhan, 430010,

11 China

12

13 *Corresponding author. Email: slguo@whu.edu.cn

14 **Abstract:** Studies on the hydrological response to continuous extreme and asymptotic
15 climate change can improve our ability to [cope with](#) the intensified water-related
16 problems. Most of the literature focused on the runoff response to climate change, while
17 neglecting the impacts of the potential variation in the catchment water storage capacity
18 (CWSC) that plays an essential role in the transfer of climate input to the catchment
19 runoff. This study aims to systematically identify the response of the CWSC to the long-
20 term meteorological drought and asymptotic climate change. Firstly, the time-varying
21 parameter is derived to reflect the CWSC periodic/abrupt variations in both drought
22 and non-drought periods. Secondly, the change points and varying patterns of the
23 CWSC are analysed based on the Bayesian change point analysis with multiple
24 evaluation criteria. Finally, various catchment properties and climate characteristics are
25 used to explore the possible relationship between these variables and the temporal
26 variation characteristics of the CWSC. The catchments that suffered from the prolonged
27 meteorological drought in southeast Australia were selected as the case study. Results
28 indicate that: (1) the increase of amplitude change in the CWSC are observed in 83/92
29 catchments during the prolonged drought period, and significant shifts in the mean
30 value of the CWSC are detected in 77/92 catchments; (2) the median response time of
31 the CWSC for all 92 catchments with significant changes is 641.3 days; (3) the values
32 of the CWSC are changed significantly in the catchments with small areas, low
33 elevations, small slope ranges, large forest coverage, and high soil water holding
34 capacities. This study could enhance our understanding of the variations in catchment

35 property under [climate change](#).

36 **Keywords:** catchment water storage capacity; prolonged meteorological drought;
37 extreme and asymptotic climate change; southeast Australia

38 **1. Introduction**

39 Climate change [has been](#) one of the most significant drivers influencing the mechanism
40 of runoff generation and the confluence process of catchments (Jung et al.,
41 2012;Changnon and Gensini, 2019). Depending on the extent and duration of climate
42 change, it [could](#) be classified into extreme (e.g., from prolonged meteorological drought
43 to extremely wet conditions in a period) and asymptotic changes (climate change in
44 different seasons in a normal year) (Shen et al., 2018). For instance, significant
45 variations (i.e., less runoff than expected) in hydrological behaviour [have been](#) reported
46 during the decade-long millennium drought of many catchments in south-eastern
47 Australia compared with the previous wet period (Saft et al., 2016). [In addition](#),
48 seasonally asymptotic variations [have been](#) identified in many catchments in America
49 [due to the seasonal growth and die-off of vegetation](#) (Deng et al., 2018;Pan et al., 2019a),
50 Asia (Deng et al., 2016) and Australia (Pan et al., 2019b). Studies on the hydrological
51 response of catchments to different climate change scenarios not only can improve our
52 understanding of the hydrological variation mechanism of the catchment, but also
53 enhance our ability to prevent unpredictable extreme events.(Kusangaya et al.,
54 2014;Kundu et al., 2017).

55 Accordingly, studies on the hydrological response to the changing environments

56 generally included two main approaches, i.e., statistical analysis and hydrological
57 modelling. Statistical analysis methods can be used to detect trend changes of prolonged
58 hydrological and meteorological data series (Costa et al., 2003; Siriwardena et al., 2006);
59 nevertheless, they usually lack sufficient physical explanations for the potential
60 variation in catchment hydrological response (Lin et al., 2015; Liu et al., 2018).
61 Hydrological models that can comprehensively consider the spatial heterogeneity and
62 physical process of the catchment are broadly used to quantify the hydrological
63 response under multiple climate conditions (Abbaspour et al., 2007; Tu, 2009; Chen et
64 al., 2019; Tian et al., 2021). For example, Chawla and Mujumdar (2015) adopted the
65 Variable Infiltration Capacity (VIC) model to evaluate the runoff response in the upper
66 Ganga basin. Shen et al. (2018) adopted the Hydrological Model of École de
67 Technologies Supérieure (HMETS) to estimate the uncertainty of runoff response to
68 climate change. Tian et al. (2021) applied the Soil and Water Assessment Tool (SWAT)
69 model to assess the effects of climate change on future runoff in the Han River basin,
70 China. However, most of the previous studies on hydrologic response mainly focused
71 on the variations in runoff response to climate change, without paying attention to the
72 causality between the varying climates (i.e., extreme and asymptotic changes of
73 climates) and variation in catchment properties.

74 Many previous studies (McNamara et al., 2011; Melsen et al., 2016; Carrer et al.,
75 2019) indicated that the catchment water storage capacity (CWSC) is one of the most
76 significant parameters influencing the mechanism of hydrological response of

77 catchments. The CWSC is defined as ‘in an unregulated and unimpaired catchment, the
78 water storage capacity refers to the maximum volume of water stored within a
79 catchment and its distribution among groundwater, soil moisture, vegetation, surface
80 water, and snowpack, which are the variables that ultimately characterize the state of
81 the hydrological system’ (McNamara et al., 2011). The root zone storage capacity is
82 defined as “the maximum amount of soil moisture that can be accessed by vegetation
83 for transpiration” (Gao et al., 2014;Nijzink et al., 2016;Singh et al., 2020;Laurène,
84 2021). For a given catchment, the value of the CWSC should be greater than or equal
85 to the root zone storage capacity.

86 Our previous study identified the impact of meteorological drought on the CWSC
87 by investigating the changes in hydrological model parameters before and after drought
88 events (Pan et al., 2020). Results showed that significant shifts in the CWSC were
89 identified in almost two-thirds of the catchments in south-eastern Australia during the
90 prolonged meteorological drought period. Two subsets of catchments with opposite
91 response directions were identified in the study area, i.e., the subsets of catchments with
92 the reduced and increased runoff generation rates, respectively. The main potential
93 reasons may be the difference in the proportion of evergreen broadleaf forests in these
94 catchments. We only considered the average shifts from the non-drought period to the
95 drought period and treated the CWSC of each period as a constant while neglecting the
96 time-varying characteristics of the CWSC of each catchment due to the periodic climate
97 change, and thus was unable to reflect variation in catchment characteristics under

98 asymptotic climate.

99 Recently, studies of the potential time-varying CWSC characteristics based on the
100 simulation of the temporal variations of hydrological parameters have attracted a lot of
101 attention (Coron et al., 2012;Brigode et al., 2013;Patil and Stieglitz, 2015;Deng et al.,
102 2018), and provided a new approach for better representing changes in catchment
103 characteristics (Deng et al., 2016). Accordingly, the selected model parameters that
104 refer to the CWSC in the model structure were constructed as multiple hypothetical
105 functions based on physical covariates (e.g., time covariates and catchment attributes),
106 and their simulation results were evaluated and compared with observations through
107 specific criteria. Thus, the functional form that achieved the best simulation
108 performance would be recognized as the best item to represent the potential changes in
109 the catchment property (Jeremiah et al., 2013;Westra et al., 2014;Pan et al., 2019a;Pan
110 et al., 2019b).

111 In this study, we systematically explore the response of the CWSC to both extreme
112 climate changes (i.e., prolonged meteorological drought) and asymptotically periodic
113 climate changes. In particular, three scientific questions will be investigated as follows.

114 (1) What are the change characteristics of the CWSC under the conditions of
115 prolonged meteorological drought and asymptotic climate variation?

116 (2) Which catchment features and climate factors are more likely to relate to the
117 change of the CWSC?

118 (3) What is the difference in the CWSC when both extreme climate variation and

119 asymptotic climate variation are considered compared with extreme climate variation?

120 **2. Materials**

121 **2.1. Study area**

122 In this study, south-eastern Australia was selected as the initial study area. To minimize

123 the impact of human activities, 398 catchments that were not disturbed by reservoirs or

124 irrigation systems are selected in this study. The study area extends from southern

125 Victoria to New South Wales and Queensland. The study area and the locations of the

126 398 initial catchments is illustrated in [Fig. 1](#). [Saft et al. \(2015\)](#) and [Pan et al. \(2019b\)](#)

127 indicated that these catchments had experienced about ten years of meteorological

128 drought near the millennium, which had a significant impact on the stability of local

129 ecosystems and the development of society, economy, and politics (Nicholls, 2004; Hunt,

130 [2009](#); [Potter et al., 2011](#); [Hughes et al., 2012](#); [van Dijk et al., 2013](#); [Saft et al., 2015](#)).

131 The essential climate characteristics include the large proportion of arid areas, the

132 semi-annual distribution of annual precipitation, and the terrain, geology, land cover,

133 and climate conditions are differentiated between various state catchments. The annual

134 mean precipitation and temperature range from 507 mm to 1814 mm and 8.26°C to

135 19.52°C, respectively. From the perspective of spatial and temporal distribution, the

136 precipitation in the catchments of Victoria state is mainly concentrated in winter. In

137 contrast, the northern catchments in New South Wales and Queensland states have more

138 rain in summer than in winter. The potential reason for this phenomenon is ENSO (El

139 Niño-Southern Oscillation). In terms of runoff, runoff in summer is dominant in
140 northern catchments, while runoff in winter is more likely to occur in southern
141 catchments.

142 **2.2. Data set**

143 **Table 1** summarized the description and source of the three types of data sets, which
144 includes (1) meteorological data (daily precipitation and potential evapotranspiration
145 (PET)), (2) hydrological data (daily runoff), and (3) catchment characteristics
146 (catchment area, mean elevation, mean slope, forest coverage percentage, etc).

147 398 catchments were selected by Zhang et al. (2013), with catchment areas ranging
148 from 50 km² to 17000 km². The collection period of observations of these catchments
149 ranges from 1976 to 2011. It is noted that the historical meteorological observations of
150 all catchments in the data sets were complete. However, the daily runoff observations
151 of 125 catchments were incomplete with the integrity of the time series being less than
152 80%. Thus, these catchments were excluded, and the remaining 273 catchments were
153 used for the purpose of meteorological drought identification. Finally, 145 catchments
154 were identified through a long-term meteorological drought with a drought period
155 longer than seven years. The drought periods corresponding to those 145 catchments
156 are exhibited in [Fig.2](#). Based on the identification criteria of the prolonged drought
157 period, all of the drought periods in these catchments lasted more than seven years. In
158 addition, the drought periods of 35% of the catchments spanned over thirteen years. It

159 can be found that the prolonged meteorological drought of most catchments started after
160 1990 and ended before 2009. In particular, the meteorological drought of 34 catchments
161 began in 1997, and 37 catchments began in 2001.

162 The characteristics of the 145 catchments with prolonged meteorological drought
163 (**Table 2**) demonstrate that there are significant differences in physical properties
164 among different catchments. For example, the catchment area, mean elevation, and
165 mean slope range from 54 to 6818 km², from 47 to 1351m, and from 0.3 to 13.6°,
166 respectively. The interval of forest coverage is [15%, 92%]. These catchment features
167 were selected as potential impact factors and analysed further in Section 4.3.

168 **3. Methodology**

169 The proposed methodology and procedures are sketched in **Fig.3**. To investigate the
170 response of the CWSC to the prolonged meteorological drought and asymptotic climate
171 variation, the study scheme is conducted with the following four procedures: (1)
172 identification of prolonged meteorological drought; (2) derivation of the response of
173 the CWSC to long-term meteorological drought and asymptotic climate variation based
174 on the Bayesian change point analysis and the hydrological modelling approach; and
175 (3) analysis of potential factors (i.e., properties of the catchments and climate
176 characteristics) that may be related to the potential changes of the CWSC and the
177 response time (defined as the time interval between the occurrence of the prolonged
178 meteorological drought and the abrupt shift of the CWSC).

179 **3.1. Identification of prolonged meteorological drought**

180 There are many methods/indexes, such as the Standardized Precipitation Index (SPI)
181 (Bayat et al., 2015), Rainfall Departure Analysis (Kumar et al., 2020), and Standardized
182 Precipitation-Evapotranspiration Index (SPEI) (Das et al., 2021), have been used to
183 identify the prolonged meteorological drought. Saft et al. (2015) introduced a drought
184 definition algorithm that was based on the annual rainfall only and proved to have a
185 lower degree of dependence and [more robustness](#) than other selected approaches in the
186 south-eastern Australia catchments. It is mentioned that the prolonged drought period
187 should be longer than 7 years according to the defined algorithm. For more detailed
188 information about this method, please refer to Saft et al. (2015) and Pan et al. (2019b).

189 **3.2. Hydrological model**

190 The GR4J hydrological model (modèle du Génie Rural à 4 paramètres Journalier) was
191 used to simulate the potential change characteristics of the CWSC before and after the
192 prolonged meteorological drought. The GR4J model is [a daily lumped rainfall-runoff](#)
193 [model](#) developed by Perrin et al. (2003) and improved by Le Moine et al. (2008), and
194 it has been used in more than 400 regions with various climatic characteristics around
195 the world, such as China (Zeng et al., 2019), France (Perrin et al., 2003), North America
196 (Pan et al., 2019a), and Australia (Coron et al., 2012). Its validity in the simulation of
197 rainfall-runoff relationship and reflection of potential changes in catchment properties
198 has been verified by (Le Moine et al., 2008;Simonneaux V, 2008).

199 **3.2.1 Model structure**

200 The original GR4J model framework proposed by Perrin et al. (2003) only contains
201 four parameters, and its structure is shown in **Fig.4**. The meanings of the four model
202 parameters are introduced as follows: θ_1 is the maximum capacity of the soil moisture
203 accounting storage, which is used to represent the CWSC (mm) in this study; θ_2 is the
204 groundwater exchange coefficient (mm); θ_3 represents the one-day-ahead maximum
205 capacity of the routing storage (mm); and θ_4 is the time base of unit hydrograph UH1
206 (day). All model parameters are real values, θ_1 , θ_3 and θ_4 are positive, and θ_2 can be
207 positive, negative, or 0.

208 Based on the existing data and catchment attributes, it is almost impossible to
209 obtain the real value of the CWSC by current technology. However, the hydrological
210 simulation method provides a new perspective for revealing the potential changes of
211 the CWSC, i.e., we can use a specific parameter (θ_1) in the GR4J model to represent
212 the CWSC and characterize its variation in the real catchment. Similar studies can be
213 found in Westra et al. (2014), and Deng et al. (2016). Hence, the simulated values of
214 parameter θ_1 and its time-varying characteristics are used to represent the change of the
215 real CWSC. It should be noted that θ_2 , θ_3 and θ_4 are assumed to remain constant; similar
216 parameter settings can be found in previous studies (Westra et al., 2014; Pan et al., 2020).

217 **3.2.2 Periodicity of the CWSC**

218 As explained, parameter θ_1 in the GR4J model was used to represent the real CWSC

219 according to its implications. Our previous work (Pan et al., 2020) verified that the
220 CWSC (i.e., parameter θ_l) had an “abrupt” point after the prolonged meteorological
221 drought, which assumes that the offset of the estimated θ_l represents the change of the
222 CWSC. Meanwhile, θ_l in each period is recognized as a constant value and does not
223 include the periodicity of the CWSC that were outlined by many previous works (Nepal
224 et al., 2017;Kunnath-Poovakka and Eldho, 2019;Sezen and Partal, 2019). However,
225 Westra et al. (2014) and Pan et al. (2020) indicated that the CWSC had periodic
226 variability that may be due to the seasonal growth and wiling of catchment vegetation.

227 In this study, the potentially periodic variation characteristics of the CWSC
228 (represented by GR4J model parameter θ_l) was included to reflect the asymptotic
229 change within different periods (i.e., periods before and after the change-point), which
230 was described by the sine function. The sine function is one of the most fundamental
231 functional forms to represent the periodic change of variables (Westra et al., 2014; Pan
232 et al., 2019a; Pan et al., 2019b). Furthermore, the potentially extreme change of the
233 CWSC between the two periods was denoted by the variations between Equations (1)
234 and (2). The time-varying functions of θ_l during two periods are presented as follows.

235 Before the change-point:

$$\theta_l = \alpha_1 \sin(\beta_l t + \gamma_l) + \delta_l \quad (1)$$

236 After the change-point:

$$\theta_l' = \alpha_2 \sin(\beta_2 t + \gamma_2) + \delta_2 \quad (2)$$

237 where, $\alpha_1, \beta_1, \gamma_1, \delta_1$ and $\alpha_2, \beta_2, \gamma_2, \delta_2$ are regression parameters for the time-varying

238 function; α_1 and α_2 signify the amplitude of the sine function; β_1 and β_2 represent the
 239 frequency of the sine function; γ_1 and γ_2 denotes the remainder in the sine function; and
 240 δ_1 and δ_2 refer to the intercept.

241 **3.2.3 Likelihood function and parameter estimation**

242 **(1) Likelihood function**

243 In this study, the likelihood function for catchment i from Thiemann et al. (2001)
 244 was adopted, which is shown as follows.

$$p_i(\theta(i)/\xi(i), q(i), r) \propto \left[\frac{w(r)}{\sigma} \right]^T \exp \left[-i(r) \sum_{t=1}^T \left| \frac{e_t(\theta(i))}{\sigma} \right|^{2/(1+r)} \right] \cdot p(\theta(i)) \quad (3)$$

$$\omega(r) = \frac{\{\Gamma[3(1+r)/2]\}^{1/2}}{(1+r)\{\{\Gamma[(1+r)/2]\}^{3/2}\}}, \beta(r) = \left\{ \frac{\Gamma[3(1+r)/2]}{\Gamma[(1+r)/2]} \right\}^{1/(1+r)} \quad (4)$$

245 where p means the probability of likelihood. $\theta(i) = (\theta_1, \theta_2, \theta_3, \theta_4)$; $\Gamma(\cdot)$ denotes the
 246 gamma function; T is the number of time steps; q represents the measured runoff; ξ
 247 denotes the climate variable entered into the hydrological model; e_t refers to the residual
 248 error at time step t ; and r is the type of the residual-error model (in this study, r is
 249 represented by Gaussian distribution). When verifying the model type of the residual,
 250 parameters $\omega(r), \beta(r)$ are constant values as r is certain. In addition, the prior
 251 distribution of all unknown quantities is the uniform distribution.

252 **(2) Parameter estimation**

253 The posterior distribution of all unknown variables was estimated using the
254 Shuffled complex evolution metropolis (SCEM-UA) algorithm, which was based on
255 the Markov chain Monte Carlo method (Vrugt et al., 2003; Ajami et al., 2007). For the
256 convergence of parameters, the Gelman-Rubin convergence value was selected as the
257 evaluation standard, and the convergence threshold was 1.2. The pre-set ranges of all
258 parameters are shown in **Table 3**.

259 **3.3 Change point analysis of CWSC**

260 **3.3.1 Bayesian change point analysis**

261 The Bayesian change point analysis is one of the strongest ways available to explore
262 the possible change time of the CWSC (Carlin et al., 1992; Cahill et al., 2015). The
263 likelihood probability was used to evaluate the possibility of each potential change
264 point. The most likely time point of each potential scheme is regarded as the ultimate
265 change point of that catchment.

266 **3.3.2 Criteria for evaluating significant changes in CWSC**

267 To evaluate whether the CWSC changed significantly under climate change, the
268 following three criteria were adopted.

269 **(1) The Nash-Sutcliffe efficiency coefficient**

270 To guarantee the reasonable simulation results of the GR4J model, the Nash-
271 Sutcliffe efficiency (NSE) coefficient values before and after the change point should

272 be greater than 0.6. Furthermore, the difference in NSE values between the two periods
273 should be less than $|\pm 20\%|$.

274 **(2) The minimum requirements for significant changes in storage capacity**

275 The change rate of the estimated parameter $\theta_1 (\theta'_1)$ before and after the change

276 point should exceed $|\pm 20\%|$. i.e., $\left| \frac{\theta'_1 - \theta_1}{\theta_1} \right| \times 100\% \geq 20\%$.

277 **(3) Robustness requirements of the results**

278 The initial values of model parameters were created three times to reduce their
279 impacts on the final simulation results. Moreover, only the catchments that have
280 significant changes in computation results will be taken as the final change items. If the
281 simulation results meet such robustness requirements, the results would have the lowest
282 dependency and the strongest stability on the adopted algorithm and model.

283 **3.4. Response time of a catchment**

284 Van Lanen et al. (2013) and Huang et al. (2017) showed that the recharge between the
285 groundwater and surface runoff would alleviate the hydrological response under short-
286 term meteorological drought. In other words, groundwater would buffer the surface
287 runoff during the drought period. If the duration of the meteorological drought was
288 longer than several years or even decades, the hydraulic connection between the surface
289 runoff and the underground runoff would be weak due to the gradual decrease of
290 groundwater level. For example, Pan et al. (2020) indicated that the CWSC may change

291 with the occurrence of the prolonged meteorological drought, and the potential reasons
292 were the [difference in soil composition](#) and the extensive death of vegetation during the
293 drought period. It also should be noted that the CWSC would not change immediately
294 after the occurrence of the meteorological drought but respond after a period due to the
295 existence of catchment elasticity (e.g., the existence of the hydraulic connection
296 between surface runoff and groundwater). Thus, the time interval between the
297 occurrence of the meteorological drought and the change point of the CWSC is named
298 the catchment response time.

299 **3.5 Potential factors associated with the changes in CWSC**

300 The process that leads to the change of the CWSC cannot be measured directly, so some
301 measurable factors are used to probe the lurking correlation between the change of the
302 CWSC and the catchment response time. We select 33 potential factors of catchments
303 and list them in **Table 4**, which includes 9 catchment features and 24 local climate
304 variables. It is noted that because of the limitation of available data for catchment
305 characteristics, only one static/constant value of the catchment features (A1-A9) was
306 used for the correlation analysis. Furthermore, climate variables in four time scales
307 were used, including daily (B1-B4), monthly (B5-B7), seasonal (B8-B15), and annual
308 (B16-B24) variables.

309 **4. Results**

310 **4.1 Change pattern of the CWSC**

311 The most likely change point was confirmed when three criteria had been satisfied. The
312 changing pattern of the CWSC was determined by Equations (1) and (2). In other words,
313 Equation (1)/Equation (2) reflects the potential periodic/asymptotic feature during the
314 period before/after the change point. It is obvious that $\alpha_1(\alpha_2)$ and $\delta_1(\delta_2)$ are the most
315 important parameters in the regression function, which refer to the amplitude and
316 intercept of the time-varying parameter θ_1 , respectively. Furthermore, the variation
317 between δ_1 and δ_2 denotes the average difference between θ_1 and θ'_1 , reflecting the
318 potential change between the CWSC of periods before and after the change point.

319 **Table 5** presents the variation characteristics (amplitude α and intercept δ) of the
320 CWSC in the 145 studied catchments with meteorological drought in south-eastern
321 Australia. [The results showed that 36.6% of the catchments \(55 of 145 catchments\)](#)
322 were identified to violate the criteria of the maximum performance degradation and
323 result robustness, and thus were removed from further analysis. The remaining 92
324 catchments were retained as the set of catchments that satisfied the basic criteria of NSE
325 performance and resultant robustness. As presented in Equations (1) and (2), amplitude
326 α represents the range of variation in the CWSC, a larger $|\alpha|$ implies a greater variation
327 interval of the CWSC during the specific period. Significant changes in amplitude α
328 were found in 60.0% of the catchments (87 of 145 catchments) during the drought
329 period, in which 57.2% of the catchments (83 of 145 catchments) experienced a

330 significantly increased change in amplitude α while 2.8% of the catchments (4 of 145
331 catchments) had significantly decreased variation during the drought period. In addition,
332 only 3.4% of the catchments (5 of 145 catchments) experienced a non-significant
333 change in amplitude α , in which 3 (2) catchments had a slightly increase (decrease)
334 trend. It means that most of the catchments (87 of 92 catchments) experienced a
335 significant increase trend in the range of variation during the prolonged drought period
336 ([Table 5](#)), indicating an increased dramatic cyclical variation magnitude of the CWSC
337 during the transformation from the non-drought period to the prolonged drought period.

338 The regression parameter δ , which refers to the intercept/mean value of the CWSC
339 during the specific period, was used to evaluate the average difference between the
340 CWSC during two periods. [As Table 5 indicated](#): a significant increase in mean value
341 δ was identified in 84% of the catchments (77 of 145 catchments) during the drought
342 period; but no catchment was found to have a significant decrease of δ in the drought
343 period. In addition, the number of catchments with non-significant changes in δ was 15,
344 and 6.9% of the catchments (10 of 145 catchments) and 3.5% of the catchments (5 of
345 145 catchments) were identified to have a non-significant increase and decrease trend
346 during the drought period, respectively. These results illustrated that most catchments
347 (77 of 92 catchments) experienced a significant increase trend in the average CWSC
348 during the transformation from the non-drought period to the prolonged drought period,
349 indicating an increased CWSC during the latter period.

350 The spatial distribution of the 92 catchments that satisfied the criteria of NSE

351 performance and resultant robustness is presented in **Fig. 5**. As shown in **Fig. 5(a)**, 94.5%
352 of the catchments (87 of 92 catchments) were found to have a significant increase in
353 amplitude α during the drought period. Similarly, as presented in **Fig. 5(b)**, more than
354 80% of the catchments (77 of 92 catchments) were identified to have a significantly
355 increased variation in δ . [Obvious convergence](#) was found in the spatial distribution of
356 the catchments with different change forms in the amplitude of the periodic change and
357 the average variation level of the two periods. For instance, catchments with non-
358 significant change in δ were mainly concentrated in the middle part of the south region
359 of Australia. The reason for this phenomenon may be the similar physical features and
360 climatic characteristics of adjacent catchments, which result in the relatively consistent
361 change direction of catchments in a region.

362 **Fig.6** illustrates the statistical results of the change of amplitude (α) and mean
363 value (δ) between two periods (before and after the change point) in all catchments in
364 south-eastern Australia. **Figs.6(a) and 6(b)** show the absolute and relative change
365 percentage of amplitude (α) between two periods, indicating that the absolute
366 differences in the amplitude between two periods, i.e., $|\alpha_2 - \alpha_1|$ are concentrated within
367 the interval of [0, 75] for 80.4% of the catchments while the relative changes
368 $(\alpha_2 - \alpha_1)/\alpha_1$ are mostly concentrated within the interval of [0, 400%] for 69.6% of the
369 catchments. The fitting curves in **Figs.6(a) and 6(b)**, which were based on the kernel
370 smoother method (Yandell, 1996), had significant positive biases, indicating that much
371 more catchments experienced an increased tendency in the variation range of periodic

372 changes of the CWSC during the drought period. **Figs.6 (c) and 6(d)** show the absolute
373 and relative change percentage of the mean value (δ), respectively, indicating that the
374 absolute change of the mean value, i.e., $|\delta_2 - \delta_1|$, are concentrated within the interval
375 of [50, 150] for 75% of the catchments while the relative change, i.e., $(\delta_2 - \delta_1) / \delta_1$, are
376 mostly concentrated within the interval of [0, 50%] for 65.2% of the catchments.
377 Similarly, the fitting curves in **Figs.6(c) and 6(d)** had remarkable positive biases as
378 well, indicating that much more catchments experienced an increased tendency in the
379 mean value of the CWSC after the change point.

380 Among the catchments with significant variation in θ_I , two types of typical
381 catchments were taken as examples to analyse the specific changes of the CWSC
382 (shown in **Fig.7**). In catchment #222206, both α_2 and δ_2 increase significantly after
383 the change point compared with α_1 and δ_1 . Based on the posterior probability of each
384 possible change point, it was found that the change probability of the CWSC was the
385 greatest on 2002/12/27. Changes in θ_I indicate that the CWSC of catchment #222206
386 tends to increase after the change point. In catchment #421042, amplitude α_2 decreases
387 significantly while mean value δ_2 increases significantly after the change point. The
388 time corresponding to the change point was 2001/7/30, which refers to the moment
389 when θ_I changes. Therefore, the above results of the two example catchments suggest
390 that the CWSC of various catchments may experience different magnitudes of change
391 under a sustained reduction in rainfall. In addition, a time lag phenomenon clearly
392 occurred between the onset of the meteorological drought and the change in θ_I .

393 **4.2 Response time of catchments with a significant change in the**
394 **CWSC**

395 As mentioned in Section 3.4, the response time refers to the time interval between the
396 occurrence of the meteorological drought and the change point of the CWSC. The
397 magnitude distribution of response time in the 92 catchments that satisfied the basic
398 criteria of NSE performance and result robustness was manifested in **Fig.8**, which
399 indicates that the response time in nearly one-third of the catchments (27/92) fell within
400 the range of 800-1000 days, followed by the response time of 17 catchments fell within
401 the range of 600-800 days. Furthermore, as shown in **Table 6**, the average and median
402 response times of the catchments with significant changes in δ are 660.7 days and 750.6
403 days, respectively. Since no significant decreased variation in δ was found, the
404 catchments with significant changes in δ after the change point [all realized a significant](#)
405 [increase trend](#). In the catchments with a [significant increase](#) in amplitude α , the average
406 and median estimates of the response time are 660.4 and 750.6 days, respectively; while
407 those of the catchments with [a significant decrease](#) in α are 391.9 and 422 days,
408 respectively. A significant difference was identified in the length of the response time
409 between two sets of catchments separately [with a significant increase and decrease](#) of
410 amplitude α . According to the results shown in **Table 6**, catchments with increased
411 variation intervals of the periodic changes generally had a longer response time.

412 **4.3 Factors for shifts in the CWSC**

413 **4.3.1 Factors for shifts in the amplitude of the CWSC**

414 To provide a better understanding of the response of the variation range of the CWSC
415 to the prolonged meteorological drought and the variation characteristics under
416 asymptotic climate change, we investigated whether the change in amplitude α was
417 associated with particular catchment features and climate inputs, i.e., are variation in
418 the CWSC more likely to occur in the catchments with certain properties? Thus, 9
419 multiple catchment features and 24 climate variables that may drive the shifts in
420 catchment response were analysed in this part.

421 Firstly, 92 catchments that satisfied the basic criteria of NSE performance and
422 result robustness were used in this part. According to the significance level of the
423 change in amplitude α , the 92 selected catchments were divided into two groups,
424 namely the significant change group and the non-significant change group, denoted as
425 $g_\alpha(S)$ and $g_\alpha(NS)$ groups, respectively. As presented in **Fig.9**, the two left columns in
426 each sub-figure refer to the corresponding catchment features of $g_\alpha(S)$ and $g_\alpha(NS)$
427 groups. $g_\alpha(S)$ denotes the group of catchments with significant changes in amplitude
428 α after the change point; while $g_\alpha(NS)$ refers to the group of catchments with non-
429 significant changes in α . As for area and elevation, the mean values of area and
430 elevation in the group with significant changes are 719 km^2 and 322m, respectively,
431 which are all lower than those (913 km^2 and 587m) of the group with non-significant
432 changes. The same phenomenon appears in the slope range, the Available Soil Water

433 Holding Capacity (AWHC) of subsoil. However, other physical features of the
434 catchment (K_s topsoil, K_s subsoil, AWHC topsoil, and Forest top soil percentage) all
435 show the opposite results. The two right columns in **Fig.9** refer to the corresponding
436 catchment features of significant increase and decrease groups. The characteristics of
437 the significant increase group are quite different from those of the significant decrease
438 group. For example, the average area of the significant increase group was 692 km^2 ,
439 which was about half of that of the significant decrease group (1299 km^2). On the whole,
440 we can reach the conclusion that: catchments with small areas, low elevations, small
441 slope ranges, large forest coverage, and high AWHC of soil may change more
442 significantly than catchments with opposite characteristics. It was likely that the
443 resilience of catchments with small areas, low elevations, small slope ranges, large
444 forest coverage, and high AWHC of soil was poor, which result in an easy change in
445 the CWSC of these catchments after the interference of the meteorological drought.

446 The relationship between the amplitude (α) change of θ_l and catchment features
447 before and after the change point (see **Fig.10**) indicate that the absolute change of
448 amplitude (α) was positively correlated with mean elevation and K_s of subsoil but
449 negatively correlated with all other catchment features (see **Fig.10(a)**). Furthermore, no
450 significant correlation was found between the absolute change of amplitude (α) and all
451 catchment features. As presented in **Fig.10(b)**, a positive association was found
452 between the relative change of amplitude (α) and the AWHC of the topsoil, while
453 negative relationship was found between the former and other catchment features. The

454 correlations between the amplitude (α) change of the CWSC and 24 climate variables
455 before and after the change point were presented in **Fig.10(c) and (d)**. A weak positive
456 correlation was found between the absolute change of amplitude (α) and all climate
457 variables. The Correlation Coefficient (CC) values of α with B6 (Cv of monthly runoff)
458 and B18 (mean annual runoff) are higher than those with other climate variables, which
459 are 0.203 and 0.174, respectively. Similarly, there was no significant correlation
460 between the relative change of amplitude (α) and all climate variables (**Fig.10(d)**).
461 Since no strong correlation was found between the amplitude (α) and a single factor,
462 we speculate that the potential change of the variation range of the CWSC was the result
463 of the combination of various catchment features and climate factors.

464 **4.3.2 Factors for the shifts in the mean value of the CWSC**

465 Similarly, we also explored the potential relationship between the change of mean value
466 (δ) of the CWSC and the catchment features/climate characteristics. According to the
467 significance level of the change in mean value δ , the 92 catchments were also divided
468 into two groups, denoted as $g_\delta(S)$ and $g_\delta(NS)$ groups. $g_\delta(S)$ denotes the group with
469 a significant change in mean value δ after the change point; while $g_\delta(NS)$ refers to the
470 group with a non-significant change in δ .

471 The two left columns in **Fig.11** present the comparison of catchment features
472 between the groups with significant change and non-significant change in the mean
473 value (δ), which demonstrates that all catchment features of the $g_\delta(S)$ group are lower
474 than those of the $g_\delta(NS)$ group. As for the change magnitude, the median estimate of

475 all catchment features in the $g_\delta(NS)$ group are lower than that of the $g_\delta(S)$ group. In
476 addition, catchments in the $g_\delta(S)$ group generally had smaller areas, lower mean
477 elevations and topsoil moisture contents than those of the $g_\delta(NS)$ group.

478 **Fig.12** illustrates the Pearson correlation between the changes (absolute change
479 and relative change) of the mean value (δ) of θ_1 and catchment features before and
480 after the change point. The absolute change of the mean value (δ) was negatively
481 correlated with both catchment features (see **Fig. 12(a)**). For instance, the highest CC
482 value was acquired by the absolute variation in δ and the Ks of topsoil (CC=-0.362),
483 subsequently followed by the AWHC of the subsoil (CC=-0.341), the Ks of subsoil
484 (CC=-0.267), and the forest percentage (CC=-0.242). As illustrated in **Fig. 12(b)**, the
485 relative change of the mean value (δ) of θ_1 was negatively correlated with all
486 catchment features (except for A3 (slope range) and A6 (AWHC of topsoil)), and both
487 correlations were weak. In general, soil and forest percentage are the variables the most
488 related to the mean value (δ). The water holding capacities of various soil types were
489 different due to the dissimilarity of void and adhesion in different soil types, which
490 directly affects the ability of the catchment to absorb and store water, thereby affecting
491 the CWSC of the catchment. Furthermore, the coverage of multiple forest percentages
492 would affect the water holding capacity and water assumption ability, resulting in
493 potential changes in the CWSC. **Figs.12(c) and 12(d)** illustrate the association between
494 the changes of the mean value (δ) and 24 climate variables before and after the change
495 point. It shows that the absolute change of the mean value (δ) has significant positive

496 correlations with B9 (mean summer precipitation, CC=0.306), B17 (annual potential
497 evapotranspiration, CC=0.306), and B19 (Annual aridity index, CC=0.421) while has
498 significant negative correlations with B8 (mean spring precipitation, CC=-0.336) and
499 B21 (Cv of annual precipitation, CC=-0.245) (**Fig.12 (c)**). Only the correlation between
500 the relative change of the mean value (δ) with B20 (Mean annual runoff index, CC=-
501 0.215) and B24 (Annual base flow ratio, CC=-0.279) are significant negative,
502 respectively (**Fig.12 (d)**).

503 **4.4 Factors for the response time of catchment**

504 The Pearson correlation coefficient between the response time with catchment
505 features and climate variables is presented in **Fig.13**, which indicates that strong
506 positive correlations were identified between the response time with A2 (mean
507 elevation, CC=0.239) and A6 (AWHC of the topsoil, CC=0.249). While a strong
508 negative correlation was found between the response time and A5 (forest coverage,
509 CC=-0.225). The potential reasons for this finding are that the increased forest coverage
510 of the catchment resulted in a larger water demand of the ecosystem, and thus cause a
511 shorter response time of the CWSC to the meteorological drought. In other words, when
512 a catchment has experienced a prolonged meteorological drought, it would respond fast
513 due to its large water demand. As for the climate variables, the absolute variations of
514 most climate variables had negative correlations with the response time (**Fig.13(b)**).
515 The CC between the absolute change of the response time with B2 (mean daily potential
516 evapotranspiration), B3 (mean T_{max}), and B13 (mean summer runoff, CC) are -0.313, -

517 0.263, and -0.27, respectively, indicating the weak relationship between the relative
518 changes of most climate variables and the response time, as shown in **Fig.13(c)**.

519 **5. Discussions**

520 **5.1 Possible reasons for different changes in the CWSC**

521 The results showed that most catchments were identified to have an increasing trend in
522 both the amplitude (α) and the mean value (δ) of the CWSC after prolonged
523 meteorological drought. According to our findings, soil type and forest coverage are
524 the variables the most related to the CWSC. The soil water holding capacities of various
525 soil types were different due to the dissimilarity of void and adhesion in different soil
526 types, which directly affects the ability of the catchment to absorb/store water, thereby
527 affecting the CWSC of the catchment. Saft et al. (2015) showed that the annual rainfall-
528 runoff relationships of many catchments changed in southeastern Australia during the
529 millennium drought (1997-2009). The prolonged meteorological drought led to the
530 continuous decrease of the groundwater level as well as a significant change in soil
531 properties. Leblanc's study for southeastern Australia showed that only two years after
532 the 2001 drought, soil moisture and surface water storage lost 80 and 12 km³,
533 respectively, and the rapid drying up reached near-steady low levels (Leblanc et al.,
534 2009). Years of drought led to an almost complete drying up of surface water resources,
535 and the hydrological drought continued even after rainfall resumed. In addition, the soil
536 types in the study area include silt loam, loam, silt, sand, sandy loam, clay and loamy

537 sand, among which silt loam and loam account for more than 80% of the total study
538 area (Pan et al., 2020). As both loam and silt loam have strong adhesion and water
539 holding capacity, they can still maintain the original soil structure state even if the soil
540 pore space increases due to long-term drought. Therefore, the combination of
541 groundwater level decline and different pre-existing soil type conditions in each
542 catchment may be one of the reasons for the different directions of change in the CWSC
543 between catchments (Hughes et al., 2012). The decline in the groundwater level may
544 lead to a gradual weakening of the hydraulic connection between surface water and
545 groundwater, resulting in the potentially more voids in the soil and thus an increase in
546 the CWSC in most catchments of the study area.

547 Furthermore, the variation of forest coverage and composition would affect the
548 water holding capacity and water assumption ability, resulting in the potential changes
549 in the CWSC. Previous studies (Fensham et al., 2009; Allen et al., 2010) showed that
550 the increased frequency, duration of drought, and heat stress associated with climate
551 change are strong factors contributing to changes in vegetation dynamics that may
552 fundamentally alter forest composition and structure in many areas. Drought-induced
553 vegetation dieback was more likely to occur in regions with relatively high densities of
554 local woody cover. Adams et al. (2012) combined the extensive literature on the
555 ecohydrological effects of tree harvesting with existing studies to propose a new and
556 relevant hypothesis. For most forests, evapotranspiration would be dramatically
557 reduced after the significant dieback of the tree cover due to drought. According to Pan

558 et al. (2020), the main land use types throughout the study area are evergreen broadleaf
559 forest, grassland, woodland, and cropland. As the evergreen broadleaf forest and
560 woodland occupied most of the study region, the notable loss of tree cover caused by
561 the prolonged meteorological drought may dramatically reduce the evapotranspiration
562 in catchments. Catchments with large coverage of evergreen broadleaf forest processed
563 the large water demand per unit area (Adams et al., 2012). For comparison, the water
564 consumption of catchments with other land use types (grassland and farmland) was less,
565 and the drought resistance ability of them was relatively stronger. It can be
566 hypothesized that in catchments with large coverage of vegetation, the occurrence of
567 the prolonged drought may intensify the competition for water demand between
568 different varieties of vegetation, promoting the survival of the vegetation types with
569 less water consumption but with higher water adoption ability. Therefore, the
570 catchments with high forest cover may lead to an increase in the CWSC.

571 **5.2 The limitations of the hydrological model**

572 The GR4J model was used to address the response of the CWSC to the prolonged
573 meteorological drought. The model processes a relatively simple structure with
574 relatively low requirements for input data, and it has been widely used in rainfall-runoff
575 simulation for small and medium-sized catchments (Dhem et al., 2010; Demirel et al.,
576 2013; Sezen et al., 2019; Kunnath et al., 2019). However, the GR4J model is
577 implemented subject to restrictions and limitations due to the inadequate description of
578 the runoff generation and flow confluence processes in the large catchments (e.g.,

579 larger than 10,000 km²). Conceptual models usually consider the entire catchment to
580 be one entity, then use empirical functional relationships or conceptual simulations to
581 describe the runoff generation and flow confluence processes, and consequently adopt
582 certain parameters with physical meanings to characterize the inhomogeneity of the
583 spatial distribution of catchment characteristics. It has been argued that conceptual
584 lumped rainfall-runoff models are far from being able to tackle the challenging problem
585 of assessing the impacts of land-use or forest variation. The GR4J model lacks a
586 physical foundation but seems to best detect changes in a basin behavior (Perrin et al.,
587 2003).

588 According to Westra et al. (2014), θ_1 is the most sensitive parameter in the GR4J
589 model and therefore was used to represent the CWSC in this study. The sine function
590 was used to reflect the periodic change of the CWSC. Further studies are necessary to
591 explore the impacts of different forms of functions on the identification and simulation
592 of the periodic variation of the CWSC.

593 **6. Conclusions**

594 This study focused on the response of the CWSC to the long-term meteorological
595 drought and asymptotic climate change systematically based on the hydrological
596 simulation method. Firstly, the time-varying parameter (the most sensitive model
597 parameter in the adopted GR4J model) was derived to reflect the CWSC periodic/abrupt
598 variations in drought and non-drought periods. Secondly, the change points and varying
599 patterns of the CWSC during the transformation from non-drought to drought periods

600 were analysed based on the Bayesian change point analysis with multiple evaluation
601 criteria. Finally, a variety of catchment features and climate characteristics were used
602 to explore the possible relationship between these variables and the temporal variation
603 characteristics of the CWSC. Catchments that suffered from the prolonged
604 meteorological drought in southeast Australia were selected as the case study. The main
605 conclusions were summarized as follows.

606 (1) The increase of CWSC amplitude change was observed in 83/92 catchments
607 during the prolonged drought period, and the significant shifts in the mean value of the
608 CWSC were detected in 77/92 catchments.

609 (2) The median response time of the CWSC for all 92 catchments with significant
610 changes was 641.3 days. Specifically, the response time in 27 and 17 catchments fell
611 within the ranges of 800-1000 days and 600-800 days, respectively.

612 (3) The CWSC changed significantly in the catchments with small areas, low
613 elevations, small slope ranges, large forest coverage, and high soil water holding
614 capacities.

615 In this study, the response characteristics of the CWSC to the prolonged
616 meteorological drought in southeastern Australia were analyzed. It was found that the
617 catchment response time and mode are greatly different. However, only the correlations
618 between the changes of parameter θ_I , response time, and single-factor of catchment
619 features and climate variables were considered in this study. Subsequent studies could
620 be conducted by combining data from multiple sources to carry out multi-factor

621 regression analysis. Nevertheless, this study could enhance our understanding of the
622 variations in catchment property under [climate change](#).

623 **Acknowledgments**

624 This study was supported by the National Key Research and Development Program of
625 China (2021YFC3200303) and the National Natural Science Foundation of China
626 (Grant No. U20A20317). The numerical calculations were done on the supercomputing
627 system in the Supercomputing Center of Wuhan University. The authors would like to
628 thank the editor and anonymous reviewers for their comments, which helped improve
629 the quality of the paper.

630 **Author contributions**

631 All of the authors helped to conceive and design the analysis. Jing Tian and Zhengke
632 Pan performed the analysis and wrote the paper. Shenglian Guo, Jun Wang and Yanlai
633 Zhou contributed to the writing of the paper and made comments.

634 **Code/Data availability**

635 The data and codes that support the findings of this study are available from the
636 corresponding author upon reasonable request.

637 **Compliance with ethical standards**

638 **Conflict of interest:** The authors declare that they have no conflict of interest.

639 **References**

640 Abbaspour, K. C., Yang, J., Maximov, I., Siber, R., Bogner, K., Mieleitner, J., Zobrist, J., and Srinivasan,

641 R.: Modelling hydrology and water quality in the pre-alpine/alpine Thur watershed using SWAT, *J.
642 Hydrol.*, 333, 413-430, 10.1016/j.jhydrol.2006.09.014, 2007.

643 Adams, H. D., Luce, C. H., Breshears, D. D., Allen, C. D., Weiler, M., Hale, V. C., Smith, A. M. S., and
644 Huxman, T. E.: Ecohydrological consequences of drought- and infestation- triggered tree die-off:
645 insights and hypotheses, *Ecohydrology*, 5, 145-159, 10.1002/eco.233, 2012.

646 Ajami, N. K., Duan, Q. Y., and Sorooshian, S.: An integrated hydrologic Bayesian multimodel
647 combination framework: Confronting input, parameter, and model structural uncertainty in
648 hydrologic prediction, *Water Resour. Res.*, 43, 10.1029/2005wr004745, 2007.

649 Allen, C. D., Macalady, A. K., Chenchouni, H., Bachelet, D., McDowell, N., Vennetier, M., Kitzberger,
650 T., Rigling, A., Breshears, D. D., Hogg, E. H., Gonzalez, P., Fensham, R., Zhang, Z., Castro, J.,
651 Demidova, N., Lim, J. H., Allard, G., Running, S. W., Semerci, A., and Cobb, N.: A global overview
652 of drought and heat-induced tree mortality reveals emerging climate change risks for forests, *For.
653 Ecol. Manage.*, 259, 660-684, 10.1016/j.foreco.2009.09.001, 2010.

654 Bayat, B., Nasseri, M., and Zahraie, B.: Identification of long-term annual pattern of meteorological
655 drought based on spatiotemporal methods: evaluation of different geostatistical approaches, *Nat.
656 Hazards*, 76, 515-541, 10.1007/s11069-014-1499-3, 2015.

657 Brigode, P., Oudin, L., and Perrin, C.: Hydrological model parameter instability: A source of additional
658 uncertainty in estimating the hydrological impacts of climate change?, *J. Hydrol.*, 476, 410-425,
659 10.1016/j.jhydrol.2012.11.012, 2013.

660 Cahill, N., Rahmstorf, S., and Parnell, A. C.: Change points of global temperature, *Environ. Res. Lett.*,
661 10, 10.1088/1748-9326/10/8/084002, 2015.

662 Carlin, B. P., Gelfand, A. E., and Smith, A. F. M.: Hierarchical bayesian-analysis of changepoint
663 problems, *J. R. Stat. Soc. C-Appl.*, 41, 389-405, 10.2307/2347570, 1992.

664 Carrer, G. E., Klaus, J., and Pfister, L.: Assessing the Catchment Storage Function Through a Dual-
665 Storage Concept, *Water Resour. Res.*, 55, 476-494, 10.1029/2018wr022856, 2019.

666 Changnon, D., and Gensini, V. A.: Changing Spatiotemporal Patterns of 5-and 10-Day Illinois Heavy
667 Precipitation Amounts, 1900-2018, *J. Appl. Meteorol. Clim.*, 58, 1523-1533, 10.1175/jamc-d-18-
668 0335.1, 2019.

669 Chawla, I., and Mujumdar, P. P.: Isolating the impacts of land use and climate change on streamflow,
670 *Hydrol. Earth Syst. Sc.*, 19, 3633-3651, 10.5194/hess-19-3633-2015, 2015.

671 Chen, Q. H., Chen, H., Wang, J. X., Zhao, Y., Chen, J., and Xu, C. Y.: Impacts of Climate Change and
672 Land-Use Change on Hydrological Extremes in the Jinsha River Basin, *Water*, 11,
673 10.3390/w11071398, 2019.

674 Coron, L., Andreassian, V., Perrin, C., Lerat, J., Vaze, J., Bourqui, M., and Hendrickx, F.: Crash testing
675 hydrological models in contrasted climate conditions: An experiment on 216 Australian catchments,
676 *Water Resour. Res.*, 48, 10.1029/2011wr011721, 2012.

677 Costa, M. H., Botta, A., and Cardille, J. A.: Effects of large-scale changes in land cover on the discharge
678 of the Tocantins River, Southeastern Amazonia, *J. Hydrol.*, 283, 206-217, 10.1016/s0022-
679 1694(03)00267-1, 2003.

680 Das, S., Das, J., and Umamahesh, N. V.: Identification of future meteorological drought hotspots over
681 Indian region: A study based on NEX-GDDP data, *Int. J. Climatol.*, 41, 5644-5662,
682 10.1002/joc.7145, 2021.

683 Demirel, M. C., Booij, M. J., and Hoekstra, A. Y.: Effect of different uncertainty sources on the skill of
684 10 day ensemble low flow forecasts for two hydrological models, *Water Resour. Res.*, 49, 4035-
685 4053, 10.1002/wrcr.20294, 2013.

686 Deng, C., Liu, P., Guo, S. L., Li, Z. J., and Wang, D. B.: Identification of hydrological model parameter
687 variation using ensemble Kalman filter, *Hydrol. Earth Syst. Sc.*, 20, 4949-4961, 10.5194/hess-20-
688 4949-2016, 2016.

689 Deng, C., Liu, P., Wang, D. B., and Wang, W. G.: Temporal variation and scaling of parameters for a
690 monthly hydrologic model, *J. Hydrol.*, 558, 290-300, 10.1016/j.jhydrol.2018.01.049, 2018.

691 Fensham, R. J., Fairfax, R. J., and Ward, D. P.: Drought-induced tree death in savanna, *Global Change
692 Biol.*, 15, 380-387, 10.1111/j.1365-2486.2008.01718.x, 2009.

693 Gao, H., Hrachowitz, M., Schymanski, S. J., Fenicia, F., Sriwongsitanon, N., and Savenije, H. H. G.:
694 Climate controls how ecosystems size the root zone storage capacity at catchment scale, *Geophys.
695 Res. Lett.*, 41, 7916-7923, 10.1002/2014gl061668, 2014.

696 Huang, S. Z., Li, P., Huang, Q., Leng, G. Y., Hou, B. B., and Ma, L.: The propagation from meteorological
697 to hydrological drought and its potential influence factors, *J. Hydrol.*, 547, 184-195,
698 10.1016/j.jhydrol.2017.01.041, 2017.

699 Hughes, J. D., Petrone, K. C., and Silberstein, R. P.: Drought, groundwater storage and stream flow
700 decline in southwestern Australia, *Geophys. Res. Lett.*, 39, 10.1029/2011gl050797, 2012.

701 Hunt, B. G.: Multi-annual dry episodes in Australian climatic variability, *Int. J. Climatol.*, 29, 1715-1730,
702 10.1002/joc.1820, 2009.

703 Jeremiah, E., Marshall, L., Sisson, S. A., and Sharma, A.: Specifying a hierarchical mixture of experts
704 for hydrologic modeling: Gating function variable selection, *Water Resour. Res.*, 49, 2926-2939,
705 10.1002/wrcr.20150, 2013.

706 Jung, I. W., Moradkhani, H., and Chang, H.: Uncertainty assessment of climate change impacts for
707 hydrologically distinct river basins, *J. Hydrol.*, 466, 73-87, 10.1016/j.jhydrol.2012.08.002, 2012.

708 Kumar, A., Panda, K. C., Nafil, M., and Sharma, G.: Identification of meteorological drought
709 characteristics and drought year based on rainfall departure analysis, *J. Appl. Sci. Technol.*, 51-59,
710 2020.

711 Kundu, S., Khare, D., and Mondal, A.: Individual and combined impacts of future climate and land use
712 changes on the water balance, *Ecol. Eng.*, 105, 42-57, 10.1016/j.ecoleng.2017.04.061, 2017.

713 Kunnath-Poovakka, A., and Eldho, T. I.: A comparative study of conceptual rainfall-runoff models GR4J,
714 AWBM and Sacramento at catchments in the upper Godavari river basin, India, *J. Earth Syst. Sci.*,
715 128, 10.1007/s12040-018-1055-8, 2019.

716 Kusangaya, S., Warburton, M. L., van Garderen, E. A., and Jewitt, G. P. W.: Impacts of climate change
717 on water resources in southern Africa: A review, *Phys. Chem. Earth*, 67-69, 47-54,
718 10.1016/j.pce.2013.09.014, 2014.

719 Laurène, J. E., Bouaziz, Aalbers, E. E., Weerts, A.H., Hegnauer, M., and Hrachowitz, M.: The importance
720 of ecosystem adaptation on hydrological model predictions in response to climate change, *Hydrol.
721 Earth Syst. Sc.*, 2021.

722 Le Moine, N., Andreassian, V., and Mathevet, T.: Confronting surface- and groundwater balances on the
723 La Rochefoucauld-Touvre karstic system (Charente, France), *Water Resour. Res.*, 44,
724 10.1029/2007wr005984, 2008.

725 Leblanc, M. J., Tregoning, P., Ramillien, G., Tweed, S. O., and Fakes, A.: Basin-scale, integrated
726 observations of the early 21st century multiyear drought in southeast Australia, *Water Resour. Res.*,
727 45, 10.1029/2008wr007333, 2009.

728 Lin, B. Q., Chen, X. W., Yao, H. X., Chen, Y., Liu, M. B., Gao, L., and James, A.: Analyses of landuse
729 change impacts on catchment runoff using different time indicators based on SWAT model, *Ecol.*
730 *Indicators*, 58, 55-63, 10.1016/j.ecolind.2015.05.031, 2015.

731 McNamara, J. P., Tetzlaff, D., Bishop, K., Soulsby, C., Seyfried, M., Peters, N. E., Aulenbach, B. T., and
732 Hooper, R.: Storage as a metric of catchment comparison, *Hydrol. Process.*, 25, 3364-3371,
733 10.1002/hyp.8113, 2011.

734 Melsen, L., Teuling, A., Torfs, P., Zappa, M., Mizukami, N., Clark, M., and Uijlenhoet, R.:
735 Representation of spatial and temporal variability in large-domain hydrological models: case study
736 for a mesoscale pre-Alpine basin, *Hydrol. Earth Syst. Sc.*, 20, 2207-2226, 10.5194/hess-20-2207-
737 2016, 2016.

738 Nepal, S., Chen, J., Penton, D. J., Neumann, L. E., Zheng, H. X., and Wahid, S.: Spatial GR4J
739 conceptualization of the Tamor glaciated alpine catchment in Eastern Nepal: evaluation of GR4JSG
740 against streamflow and MODIS snow extent, *Hydrol. Process.*, 31, 51-68, 10.1002/hyp.10962, 2017.

741 Nicholls, N.: The changing nature of Australian droughts, *Clim. Change*, 63, 323-336,
742 10.1023/B:CLIM.0000018515.46344.6d, 2004.

743 Nijzink, R., Hutton, C., Pechlivanidis, I., Capell, R., Arheimer, B., Freer, J., Han, D., Wagener, T.,
744 McGuire, K., Savenije, H., and Hrachowitz, M.: The evolution of root-zone moisture capacities
745 after deforestation: a step towards hydrological predictions under change?, *Hydrol. Earth Syst. Sc.*,
746 20, 4775-4799, 10.5194/hess-20-4775-2016, 2016.

747 Pan, Z. K., Liu, P., Gao, S. D., Cheng, L., Chen, J., and Zhang, X. J.: Reducing the uncertainty of time-
748 varying hydrological model parameters using spatial coherence within a hierarchical Bayesian
749 framework, *J. Hydrol.*, 577, 10.1016/j.jhydrol.2019.123927, 2019a.

750 Pan, Z. K., Liu, P., Gao, S. D., Xia, J., Chen, J., and Cheng, L.: Improving hydrological projection
751 performance under contrasting climatic conditions using spatial coherence through a hierarchical
752 Bayesian regression framework, *Hydrol. Earth Syst. Sc.*, 23, 3405-3421, 10.5194/hess-23-3405-
753 2019, 2019b.

754 Pan, Z. K., Liu, P., Xu, C. Y., Cheng, L., Tian, J., Cheng, S. J., and Xie, K.: The influence of a prolonged
755 meteorological drought on catchment water storage capacity: a hydrological-model perspective,
756 *Hydrol. Earth Syst. Sc.*, 24, 4369-4387, 10.5194/hess-24-4369-2020, 2020.

757 Patil, S. D., and Stieglitz, M.: Comparing Spatial and temporal transferability of hydrological model
758 parameters, *J. Hydrol.*, 525, 409-417, 10.1016/j.jhydrol.2015.04.003, 2015.

759 Perrin, C., Michel, C., and Andreassian, V.: Improvement of a parsimonious model for streamflow
760 simulation, *J. Hydrol.*, 279, 275-289, 10.1016/s0022-1694(03)00225-7, 2003.

761 Potter, N. J., Petheram, C., and Zhang, L.: Sensitivity of streamflow to rainfall and temperature in south-
762 eastern Australia during the Millennium drought, 19th International Congress on Modelling and
763 Simulation (MODSIM), Perth, Australia, 2011, WOS:000314989303087, 3636-3642, 2011.

764 Saft, M., Western, A. W., Zhang, L., Peel, M. C., and Potter, N. J.: The influence of multiyear drought on
765 the annual rainfall-runoff relationship: An Australian perspective, *Water Resour. Res.*, 51, 2444-
766 2463, 10.1002/2014wr015348, 2015.

767 Saft, M., Peel, M. C., Western, A. W., and Zhang, L.: Predicting shifts in rainfall-runoff partitioning
768 during multiyear drought: Roles of dry period and catchment characteristics, *Water Resour. Res.*,
769 52, 9290-9305, 10.1002/2016wr019525, 2016.

770 Sezen, C., and Partal, T.: The utilization of a GR4J model and wavelet-based artificial neural network for
771 rainfall-runoff modelling, *Water Supply*, 19, 1295-1304, 10.2166/ws.2018.189, 2019.

772 Shen, M. X., Chen, J., Zhuan, M. J., Chen, H., Xu, C. Y., and Xiong, L. H.: Estimating uncertainty and
773 its temporal variation related to global climate models in quantifying climate change impacts on
774 hydrology, *J. Hydrol.*, 556, 10-24, 10.1016/j.jhydrol.2017.11.004, 2018.

775 Simonneaux V, H. L., Boulet G, et al.: Modelling runoff in the Rheraya Catchment (High Atlas, Morocco)
776 using the simple daily model GR4J., Trends over the last decades [C]//13th IWRA World Water
777 Congress, Montpellier, France., 2008.

778 Singh, C., Wang-Erlandsson, L., Fetzer, I., Rockstrom, J., and van der Ent, R.: Rootzone storage capacity
779 reveals drought coping strategies along rainforest-savanna transitions, *Environ. Res. Lett.*, 15,
780 10.1088/1748-9326/abc377, 2020.

781 Siriwardena, L., Finlayson, B. L., and McMahon, T. A.: The impact of land use change on catchment
782 hydrology in large catchments: The Comet River, Central Queensland, Australia, *J. Hydrol.*, 326,
783 199-214, 10.1016/j.jhydrol.2005.10.030, 2006.

784 Thiemann, M., Trosset, M., Gupta, H., and Sorooshian, S.: Bayesian recursive parameter estimation for
785 hydrologic models, *Water Resour. Res.*, 37, 2521-2535, Doi 10.1029/2000wr900405, 2001.

786 Tian, J., Guo, S. L., Deng, L. L., Yin, J. B., Pan, Z. K., He, S. K., and Li, Q. X.: Adaptive optimal
787 allocation of water resources response to future water availability and water demand in the Han
788 River basin, China, *Sci. Rep.*, 11, 10.1038/s41598-021-86961-1, 2021.

789 Tu, J.: Combined impact of climate and land use changes on streamflow and water quality in eastern
790 Massachusetts, USA, *J. Hydrol.*, 379, 268-283, 10.1016/j.jhydrol.2009.10.009, 2009.

791 van Dijk, A., Beck, H. E., Crosbie, R. S., de Jeu, R. A. M., Liu, Y. Y., Podger, G. M., Timbal, B., and
792 Viney, N. R.: The Millennium Drought in southeast Australia (2001-2009): Natural and human
793 causes and implications for water resources, ecosystems, economy, and society, *Water Resour. Res.*,
794 49, 1040-1057, 10.1002/wrcr.20123, 2013.

795 Van Lanen, H. A. J., Wanders, N., Tallaksen, L. M., and Van Loon, A. F.: Hydrological drought across
796 the world: impact of climate and physical catchment structure, *Hydrol. Earth Syst. Sc.*, 17, 1715-
797 1732, 10.5194/hess-17-1715-2013, 2013.

798 Vrugt, J. A., Gupta, H. V., Bouten, W., and Sorooshian, S.: A Shuffled Complex Evolution Metropolis
799 algorithm for optimization and uncertainty assessment of hydrologic model parameters, *Water
800 Resour. Res.*, 39, 10.1029/2002wr001642, 2003.

801 Westra, S., Thyre, M., Leonard, M., Kavetski, D., and Lambert, M.: A strategy for diagnosing and
802 interpreting hydrological model nonstationarity, *Water Resour. Res.*, 50, 5090-5113,
803 10.1002/2013wr014719, 2014.

804 Yandell, B. S.: Kernel Smoothing, *Technometrics*, 38, 75-76, 1996.

805 Zeng, L., Xiong, L. H., Liu, D. D., Chen, J., and Kim, J. S.: Improving Parameter Transferability of GR4J
806 Model under Changing Environments Considering Nonstationarity, *Water*, 11, 10.3390/w11102029,
807 2019.

808 Zhang, Y. Q., Viney, N., Frost, A., Oke, A., Brooks, M., Chen, Y., and Campbell, N.: Collation of

809 Australian modeller's streamflow dataset for 780 unregulated Australian catchments, CSIRO: Water for
810 a healthy country national research flagship, 115 pp, 2013.

811

812 **Tables**

813 **Table 1.** Description of the dataset.

814

Data type	Description	Data source
Meteorological data	daily precipitation, potential evapotranspiration	
Runoff data	daily runoff data from hydrological stations	Australian Water Resources Assessment system
Catchment features	catchment area, elevation, slope, forest coverage percentage, AWHC of the soil, K_s of the soil	

815 Note: AWHC denotes the Available Soil Water Holding Capacity; K_s refers to the Saturated
816 Hydraulic Conductivity.

817

818

819 **Table 2.** Summary of the characteristics of 145 catchments with the prolonged
820 meteorological drought.

821

Number	Catchment features	Mean	Median	Minimum	Maximum
A1	Area (km ²)	711.17	363.0	54.0	6818.0
A2	Mean elevation (m)	542.57	468.0	47.0	1351.0
A3	Slope range (°)	22.18	22.6	2.1	49.9
A4	Mean slope (°)	5.49	5.0	0.3	13.6
A5	Forest coverage (%)	55.00	57.0	15.0	92.0
A6	AWHC of the topsoil (mm)	41.26	42.0	22.0	64.0
A7	AWHC of the subsoil (mm)	88.66	87.5	27.0	188.0
A8	K _s of topsoil (mm/h)	157.52	160.0	31.0	283.0
A9	K _s of subsoil (mm/h)	62.10	53.0	4.0	216.0

822

823

824

825

826

Table 3. Ranges of the initial values of GR4J model parameters.

Parameters	Meaning	Unit	Min	Max
α_1, α_2	amplitude of the sine function	/	-200	200
θ_1	β_1, β_2 frequency of the sine function	/	0	1
	γ_1, γ_2 remainder in the sine function	/	-200	200
	δ_1, δ_2 intercept of the sine function	/	-300	300
θ_2	groundwater exchange coefficient	mm	-5.0	5.0
θ_3	capacity of catchment reservoir	mm	1.0	200.0
θ_4	unit line confluence time	day	0.1	10.0

827

828

829 **Table 4.** Selected variables that may be associated with the changes in the CWSC.

830

Category	Catchment features	Category	Climate variables
A1	Area (km ²)	A6	AWHC of the topsoil (mm)
A2	Mean elevation (m)	A7	AWHC of the subsoil (mm)
A3	Slope range (°)	A8	K _s of topsoil (mm/h)
A4	Mean slope (°)	A9	K _s of subsoil (mm/h)
A5	Forest coverage (%)		
Category	Climate variables	Category	Climate variables
B1	Mean daily precipitation (mm)	B13	Mean summer runoff(mm)
B2	Mean daily potential evapotranspiration(mm)	B14	Mean autumn runoff(mm)
B3	Mean Daily T _{max} (°C)	B15	Mean winter runoff(mm)
B4	Mean Daily T _{min} (°C)	B16	Mean annual precipitation (mm)
B5	C _v of monthly precipitation	B17	Mean annual potential evapotranspiration(mm)
B6	C _v of monthly runoff	B18	Mean annual runoff(mm)
B7	Mean monthly runoff index	B19	Mean annual aridity ratio
B8	Mean spring precipitation (mm)	B20	Mean annual runoff index
B9	Mean summer precipitation (mm)	B21	C _v of annual precipitation
B10	Mean autumn precipitation (mm)	B22	C _v of annual runoff
B11	Mean winter precipitation (mm)	B23	Mean annual base flow (mm)
B12	Mean spring runoff(mm)	B24	Annual base flow ratio

831

832 **Table 5.** The change patterns of amplitude α and mean value δ in the regression
 833 function of the CWSC of catchments with a prolonged meteorological drought in south-
 834 eastern Australia.

Factors	Magnitude	Change direction	Number of catchments	Percentage
Amplitude (α)	Significant change	Increased	83	57.24%
		Decreased	4	2.76%
	Non-significant change	Increased	3	2.07%
		Decreased	2	1.38%
	Catchments that do not meet the criteria for the maximum performance degradation and result robustness		53	36.55%
	Catchments with a prolonged meteorological drought		145	100%
	Significant change	Increased	77	53.10%
		Decreased	0	0
Mean value (δ)	Non-significant change	Increased	10	6.90%
		Decreased	5	3.45%
	Catchments that do not meet the criteria of the maximum performance degradation and result robustness		53	36.55%
	Catchments with a prolonged meteorological drought		145	100%

835

836

837 **Table 6.** Response times of different groups of catchments with significant increase/
838 decrease in regression parameters δ and α .

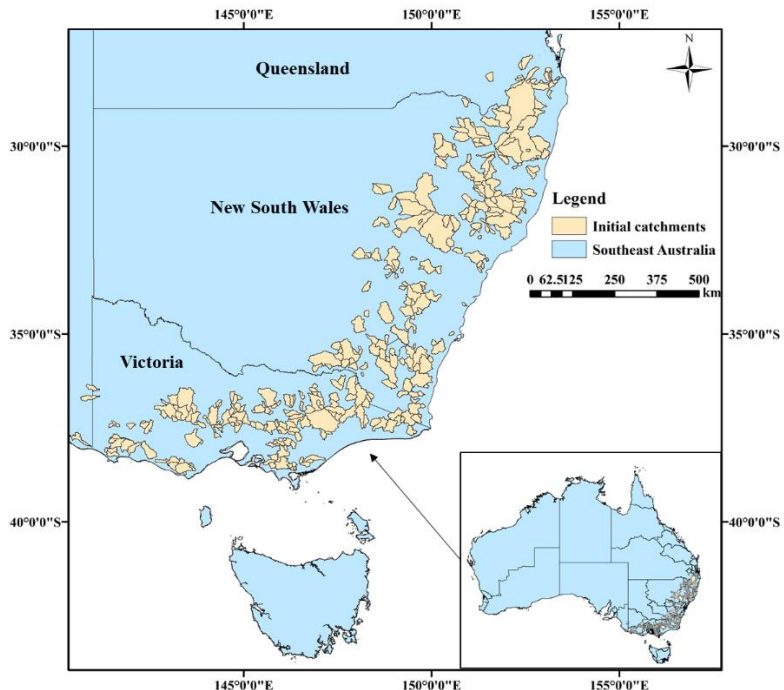
839

Catchment type	Average (day)	Median (day)	Minimum (day)	Maximum (day)
Catchments with significant increase in δ	660.7	750.6	61.8	1051.6
Catchments with significant decrease in δ	/	/	/	/
Catchments with significant increase in α	660.4	750.6	61.8	1051.6
Catchments with significant decrease in α	391.9	422	92.2	631.5

840

841 **Figures**

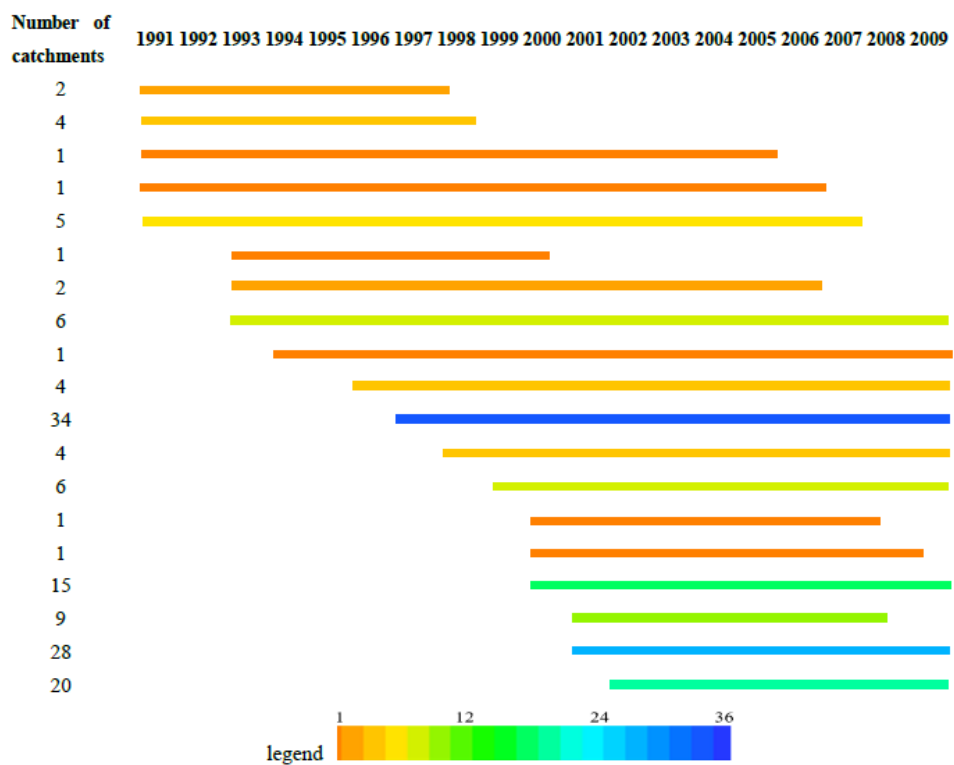
842



843

844 **Fig.1.** Spatial distribution of 398 catchments in south-eastern Australia.

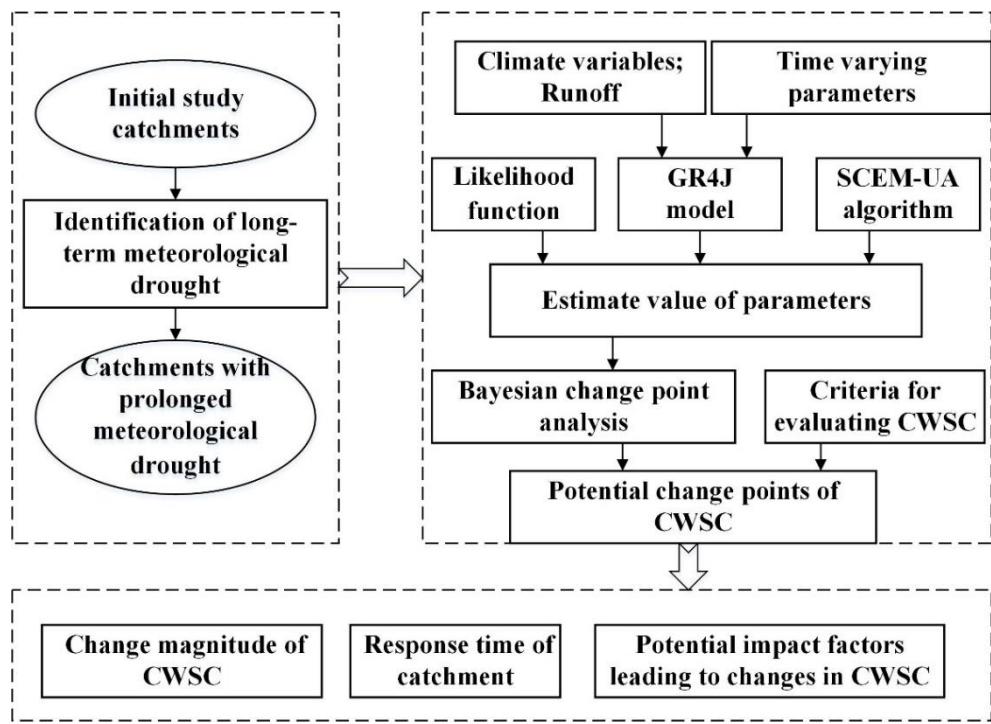
845



846

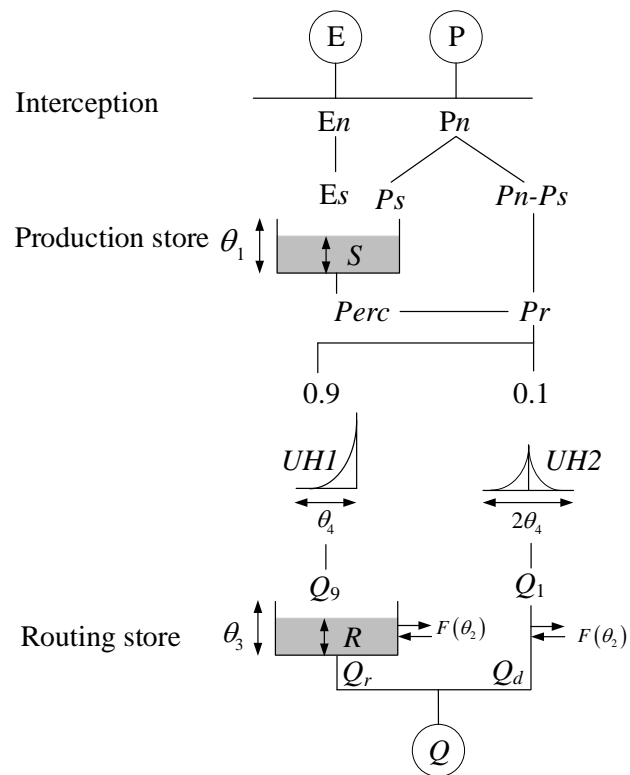
847

848 **Fig.2.** The drought periods correspond to 145 catchments with prolonged
849 meteorological drought in the south-eastern Australia.



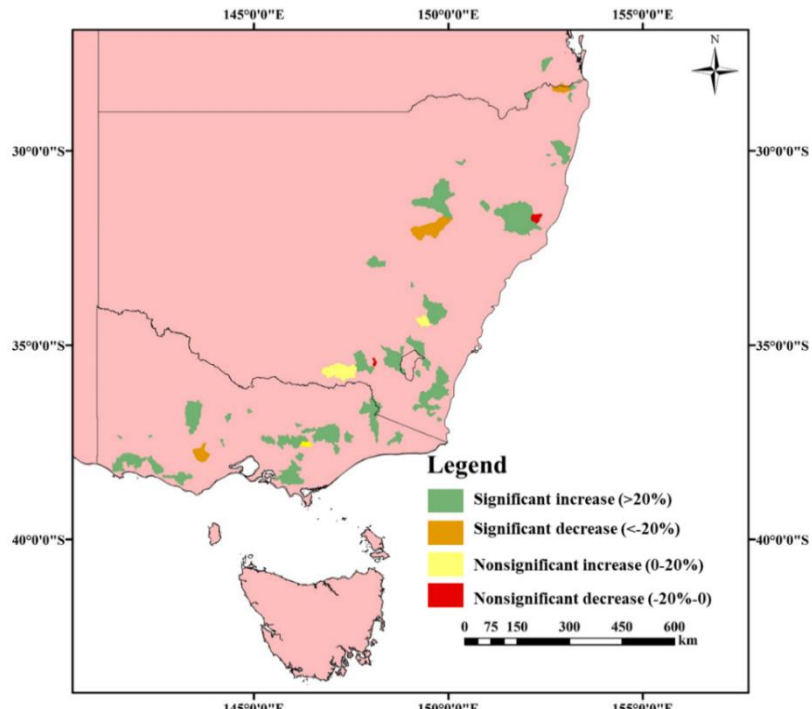
850

851 **Fig.3.** Flowchart of the proposed methodology and procedures.

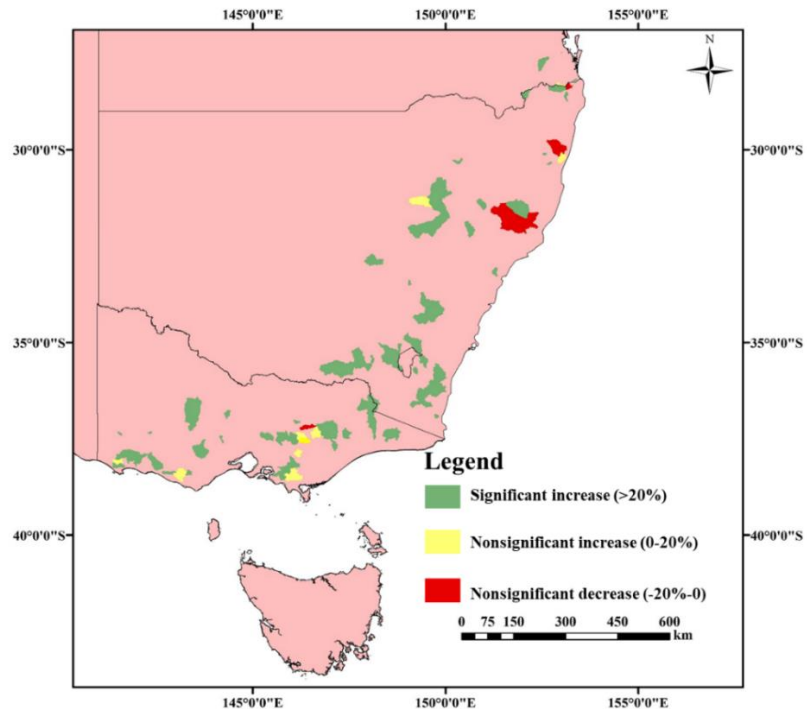


852

Fig.4. Diagram of the GR4J model proposed by Perrin et al. (2003).

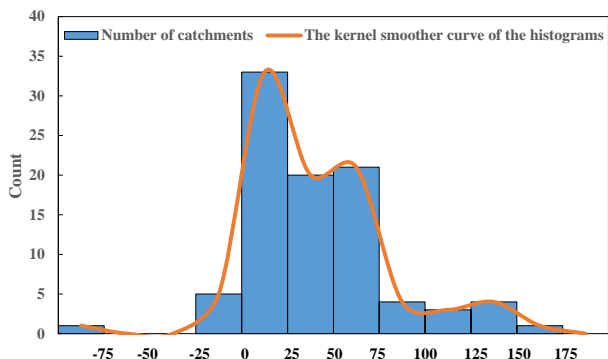


854
 855 (a) Amplitude α

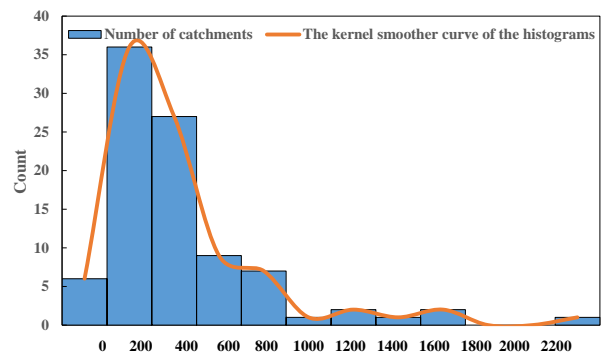


856
 857 (b) Mean value δ

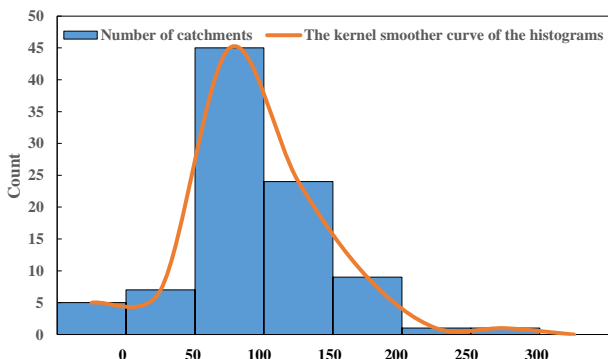
858 **Fig.5.** Spatial distribution of catchments with different change patterns in the CWSC
 859 after the prolonged drought period. (a) and (b) illustrate the spatial distribution
 860 of catchments with different variation forms in amplitude α and mean value δ
 861 during the drought period, respectively.



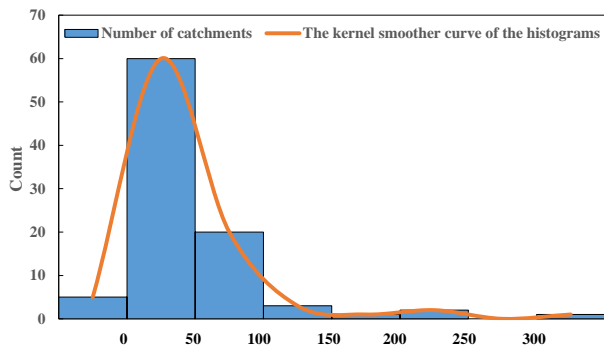
(a) Magnitude of absolute change in estimated parameter α



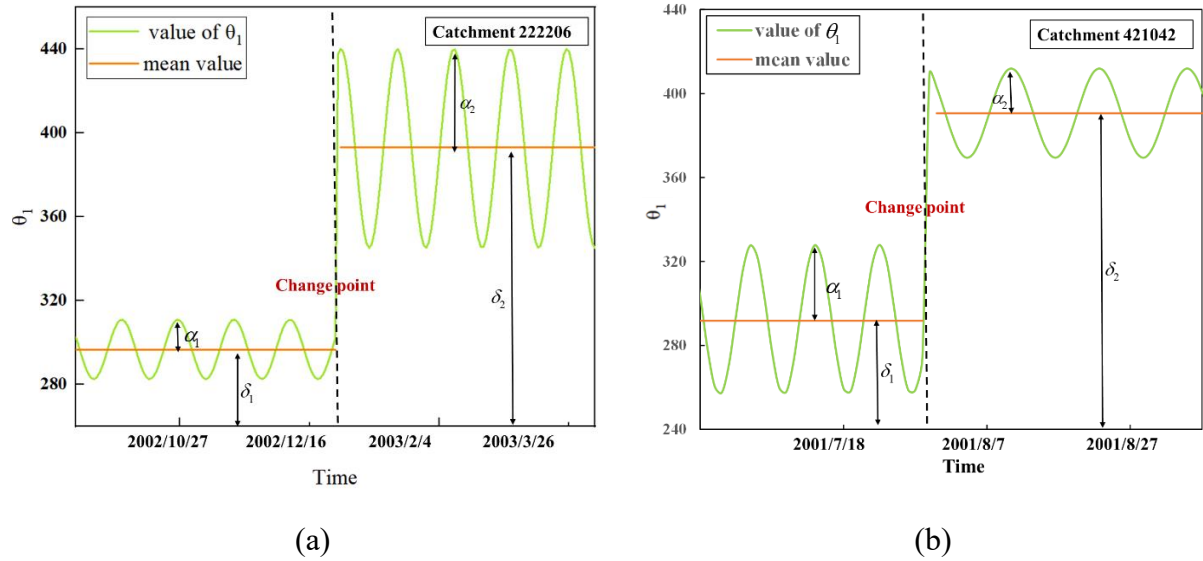
(b) Magnitude of the relative change percentage in estimated parameter α



(c) Magnitude of absolute change in estimated parameter δ



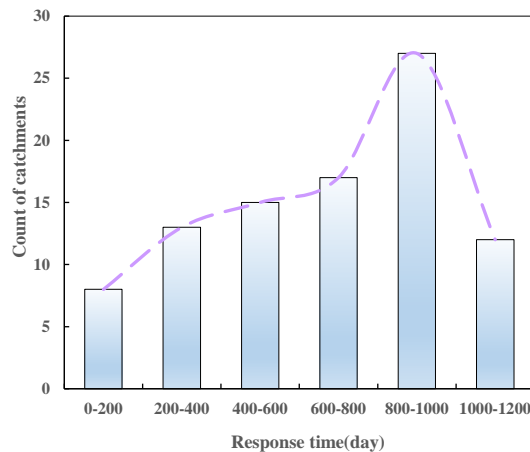
(d) Magnitude of the relative change percentage in estimated parameter δ



863

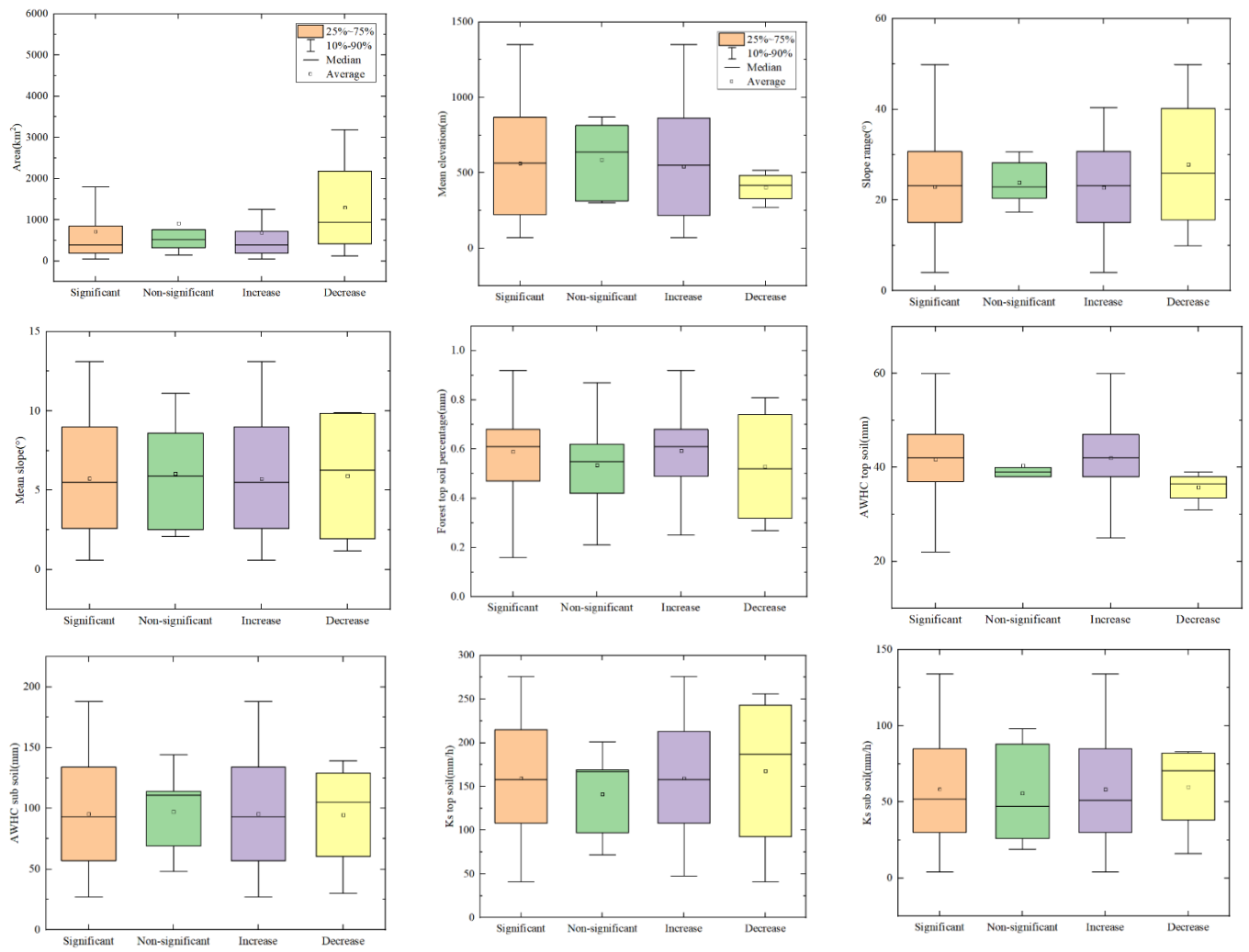
864

Fig.7. Examples of shifts in parameter θ_1 .

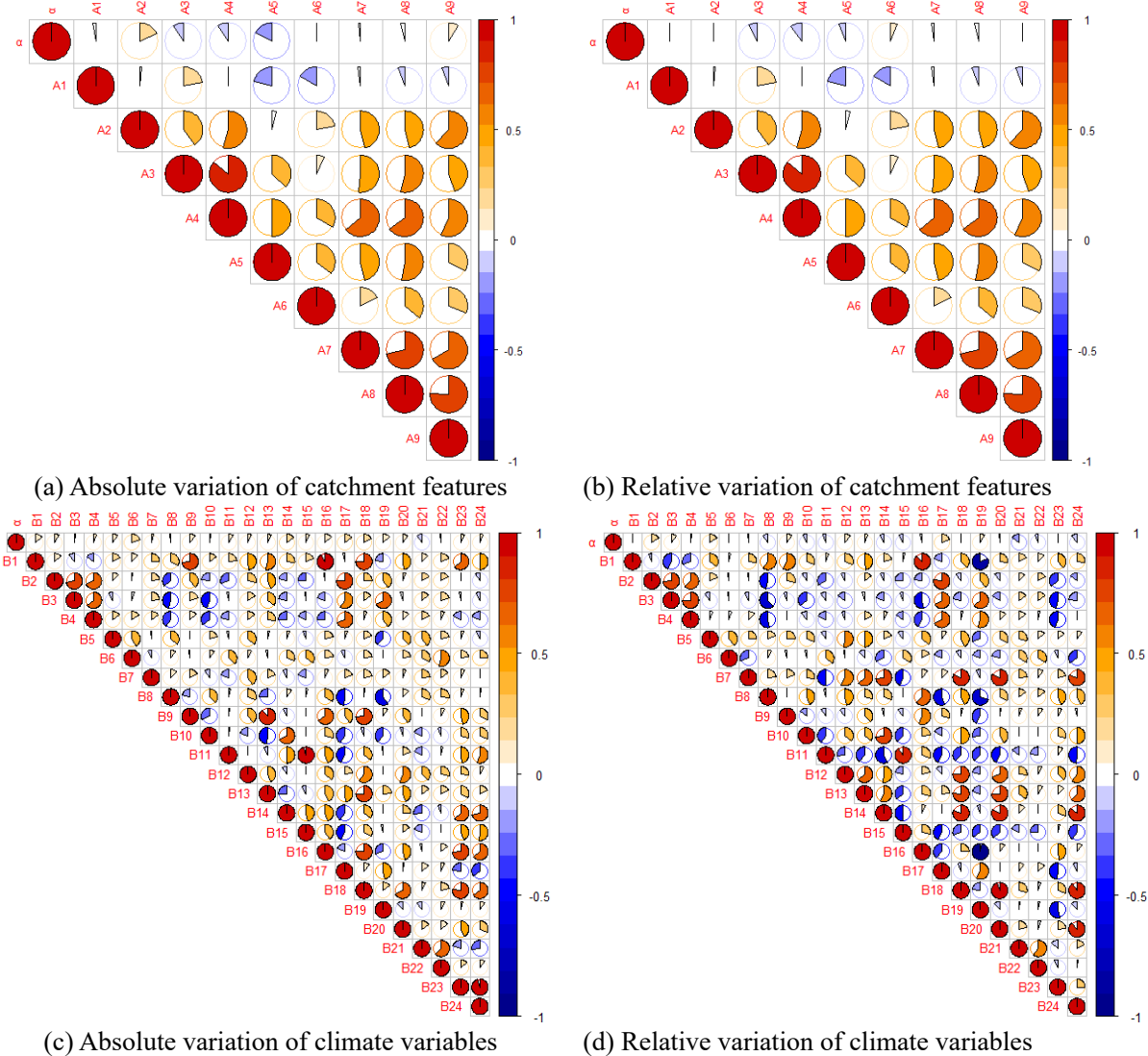


865

866 **Fig.8.** Magnitude distribution of the response time in 92 catchments that satisfied the
867 criteria for evaluating significant changes in the CWSC.



871 **Fig.9.** Physical features for the study catchments. The orange and green boxes denote
 872 the corresponding catchment features of significant increase and significant
 873 decrease groups, respectively.

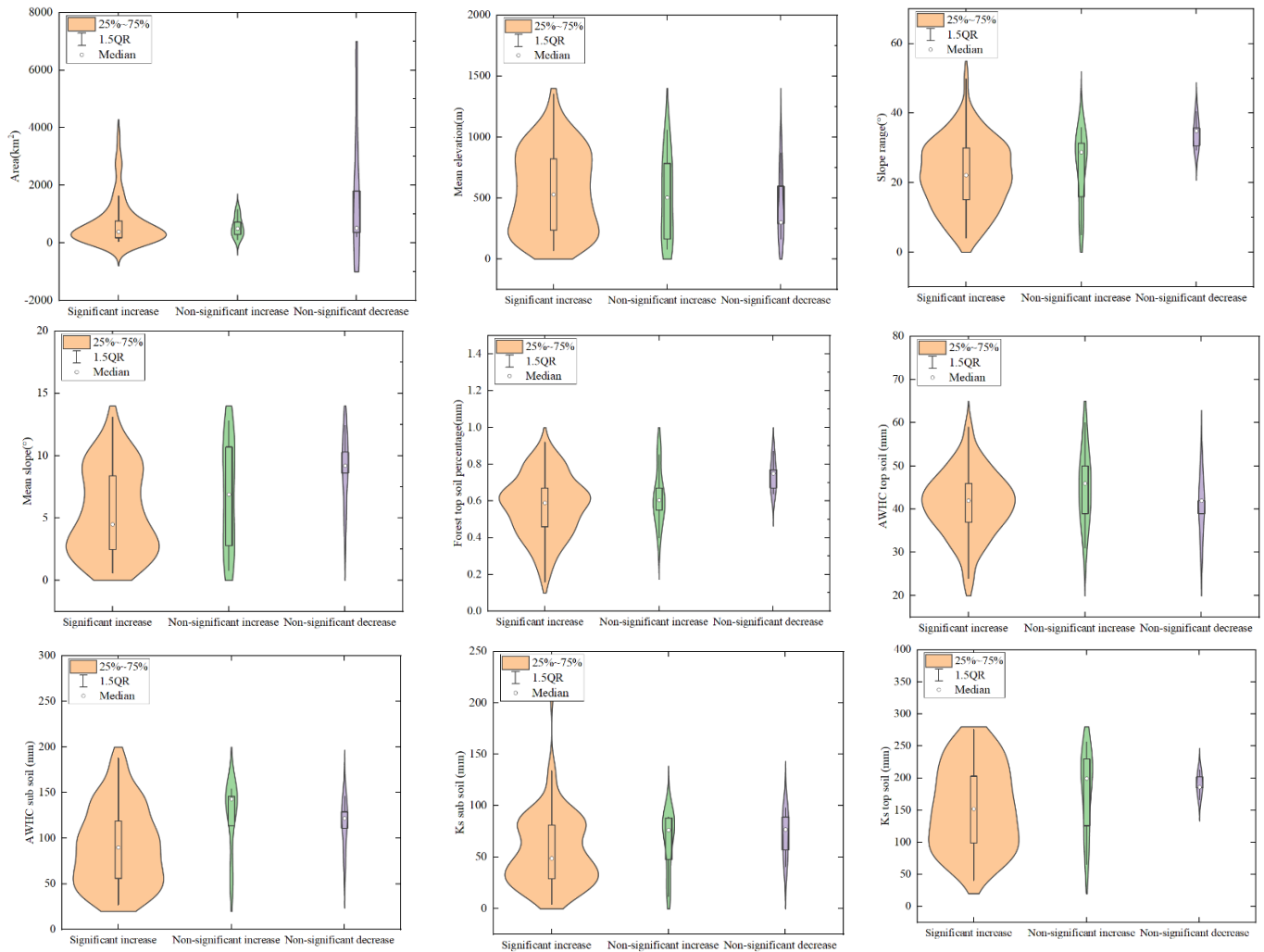


874

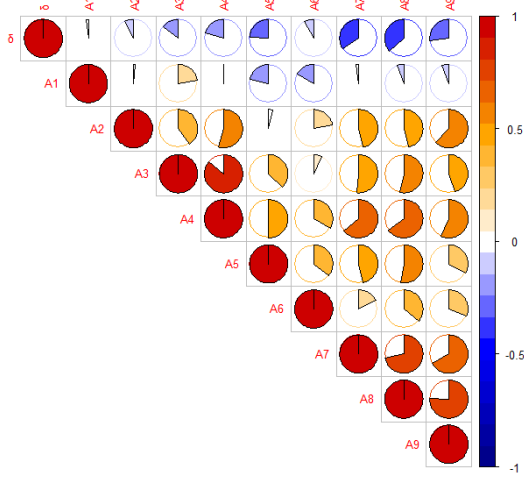
Fig.10. The Pearson correlation coefficient between amplitude (α) of θ_1 with

875

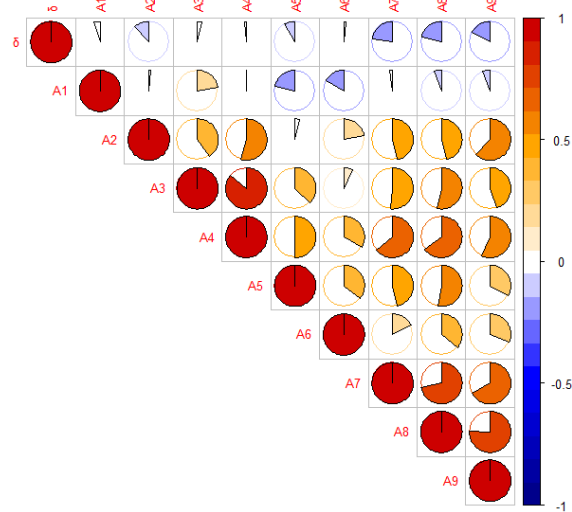
catchments features and climate variables.



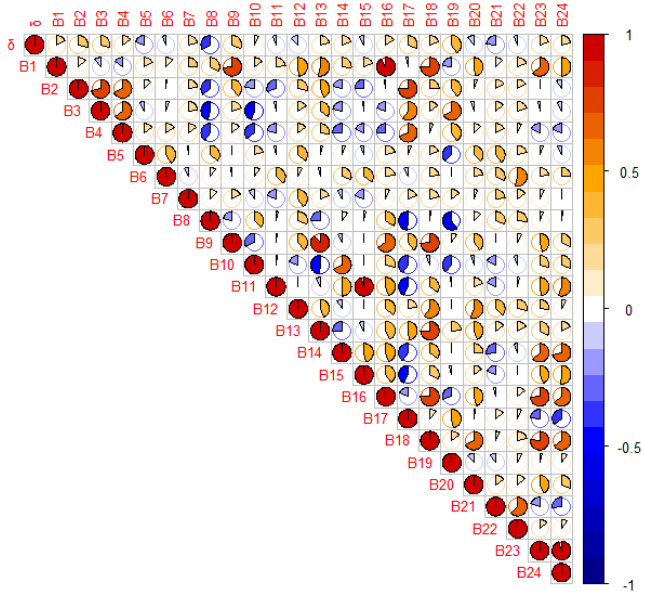
878 **Fig.11.** Comparison of catchment characteristics between the groups of catchments
 879 with significant and non-significant changes in mean value (δ).



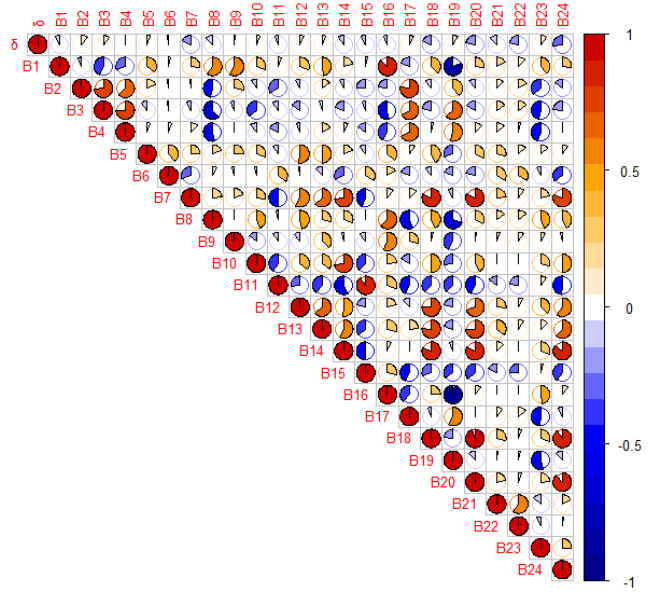
(a) Absolute variation of catchment features



(b) Relative variation of catchment features



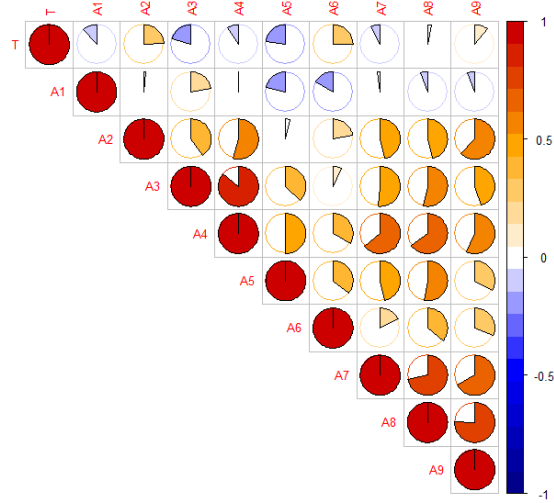
(c) Absolute variation of climate variables



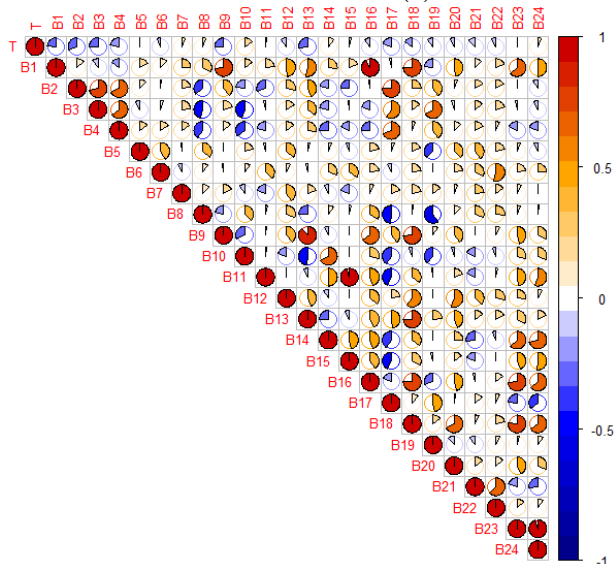
(d) Relative variation of climate variables

880

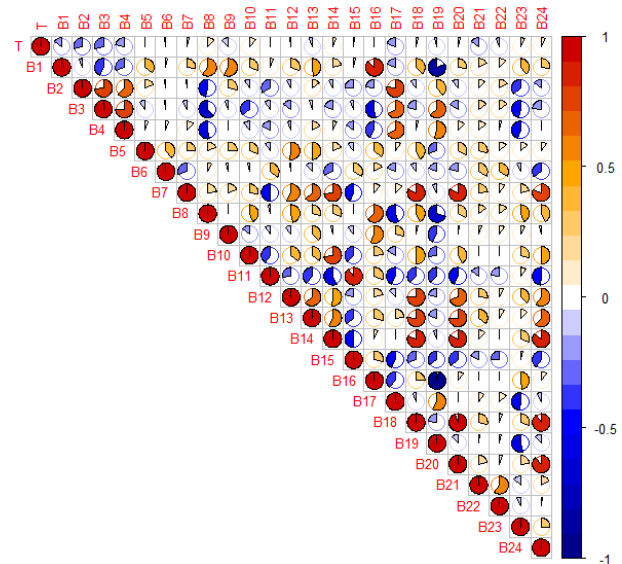
881 **Fig.12.** The Pearson correlation coefficient between the mean value (δ) of θ_1 with
882 catchment features and climate variables..



(a) Absolute variation of catchment features



(b) Absolute variation of climate variables



(c) Relative variation of climate variables

883

884 **Fig.13.** The Pearson correlation coefficient between the response time with catchment
885 features and climate variables.

886